Argonne NATIONAL LABORATORY

ANL-ART-278

Thermal Hydraulic Experimental Test Article – Fiscal Year 2023 Final Report

Nuclear Science & Engineering

About Argonne National Laboratory

Argonne is a U.S. Department of Energy laboratory managed by UChicago Argonne, LLC under contract DE-AC02-06CH11357. The Laboratory's main facility is outside Chicago, at 9700 South Cass Avenue, Argonne, Illinois 60439. For information about Argonne and its pioneering science and technology programs, see www.anl.gov.

ANL-ART-278

Thermal Hydraulic Experimental Test Article – Fiscal Year 2023 Final Report

prepared by:
Matthew Weathered, Christopher Grandy, Derek Kultgen, Edward Kent, Jordan Rein, Alex Grannan, Evan Ogren

Nuclear Science & Engineering, Argonne National Laboratory

September 2023

Executive Summary

The Thermal Hydraulic Experimental Test Article (THETA) is a facility that is used to develop sodium components and instrumentation as well as acquire experimental data for validation of reactor thermal hydraulic and safety analysis codes. The facility simulates nominal conditions as well as protected/unprotected loss of flow accidents in a sodium-cooled fast reactor (SFR). High fidelity distributed temperature profiles of the developed flow field may be acquired with Rayleigh backscatter based optical fiber temperature sensors. The facility was designed in partnership with systems code experts to tailor the experiment to ensure the most relevant and highest quality data for code validation.

THETA is comprised of a traditional primary coolant and secondary coolant system. The primary system is submerged in the pool of sodium and consists of a pump, electrically heated core, intermediate heat exchanger, and connected piping and thermal barriers (redan). The secondary system, located outside of the sodium pool, consists of a pump, sodium to air heat exchanger, and connected piping and valves.

To date a test matrix has been completed utilizing the primary system of THETA. These tests, along with computational fluid dynamics and systems code models, determined the heat transfer across the core barrel and intermediate heat exchanger outlet was too great to effectively represent scaled thermal hydraulic phenomena of a liquid metal cooled reactor. Therefore, a significant effort was made to remove the primary system from the METL 28” test vessel #4 and clean the residual sodium from the primary system to facilitate upgrades. Thermal insulation was then incorporated in the core barrel and intermediate heat exchanger outlets. The primary system was then replaced, and a series of tests were performed to assess the performance of the thermal insulation. With primary system testing and upgrades complete, the secondary system could then be brought online.

The tube side of the shell-and-tube intermediate heat exchanger was installed onto the primary system flange to begin installing the secondary system. The support structure for the secondary system was then erected on the METL mezzanine alongside the THETA primary system to facilitate installation of the secondary system components (sodium-to-air heat exchanger, flowmeter and pump). The piping and expansion tank were welded into the secondary system. Non-destructive examination of the secondary system welds was completed in order to satisfy ASME B31.3 pipe code for class M process fluids. The heating system and insulation were then added to prepare the system to be filled with sodium. The ancillary electrical equipment was installed which included the pump control box, blower VFD, pipe heater control system, etc. The secondary system will be filled, and a test matrix will be completed in early FY2024.

This page was intentionally left blank.

Table of Contents

List of Figures

List of Tables

1. Introduction

The Thermal Hydraulic Experimental Test Article (THETA) is a METL vessel experiment designed for testing and validating sodium fast reactor components and phenomena. Figure 1 to Figure 3 provide drawings and photographs of the THETA primary and secondary system. THETA possesses all the major thermal hydraulic components of a pool type sodium cooled reactor. Figure 4 provides a P&ID of the THETA primary and secondary system. THETA has been scaled using a non-dimensional Richardson number approach to represent temperature distributions during nominal and loss of flow conditions in a sodium fast reactor (SFR) [1]. THETA was designed in collaboration with systems code experts to inform the geometry and sensor placement to acquire the highest value code validation data.

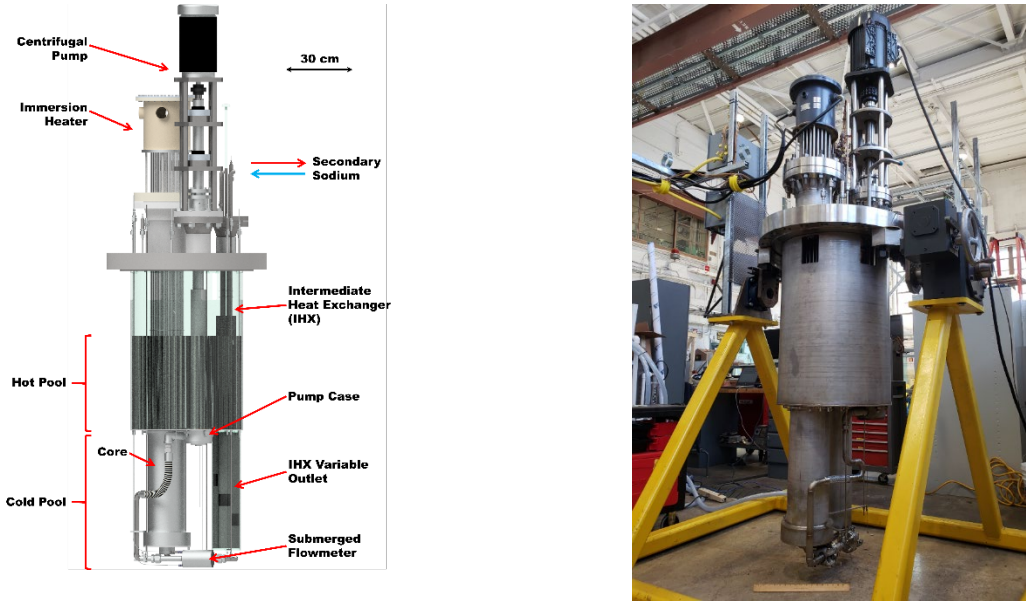

Figure 1: THETA primary system

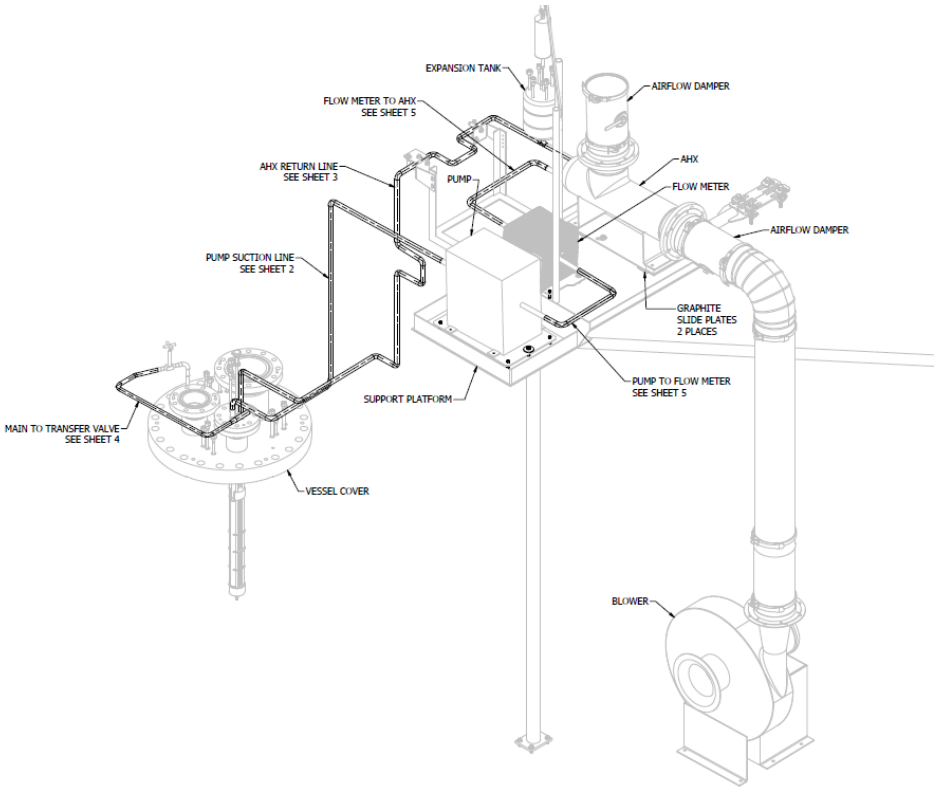

Figure 2: Isometric drawing of THETA secondary system

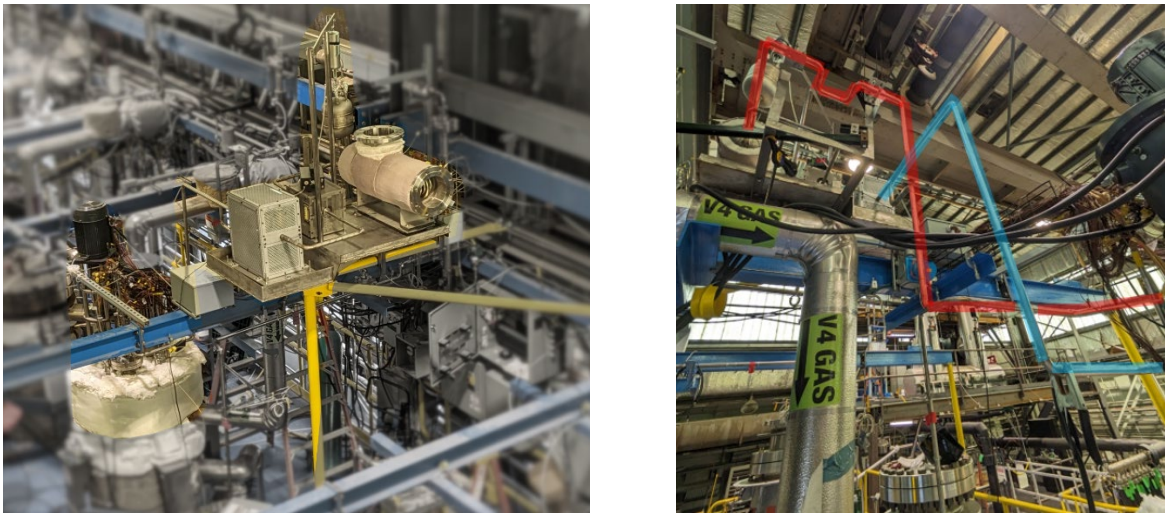

Figure 3: Photographs showing the THETA secondary system components installed on the platform structure (left) and the hot return and cold supply secondary sodium piping (right). Note the hot return and cold supply sodium pipes have been highlighted with red and blue, respectively.

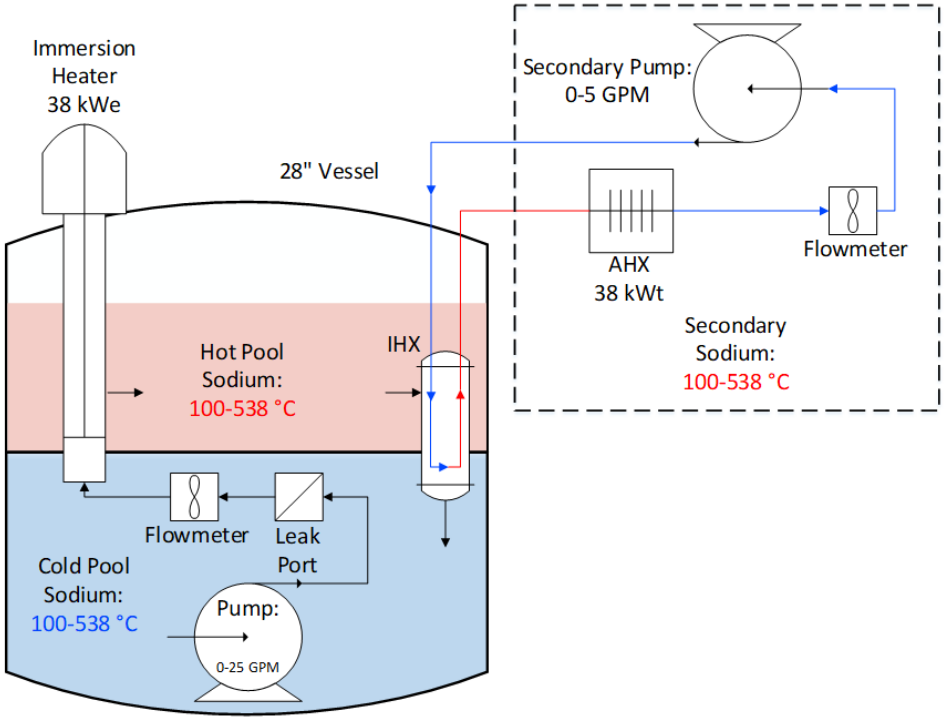

Figure 4: P&ID schematic of THETA

2. Primary System Development

2.1. Primary System Testing

2.1.1. Stratification Testing

A testing campaign was completed to acquire thermal stratification data in the primary system. A portion of the testing matrix which includes ~12 tests was included in Table 1 for reference. During these tests the pump was set to a constant speed and the hot and cold pools were brought to an isothermal condition of around 200 °C. During the entirety of the tests, the vessel heaters were either turned off or set to maintain a quasi-adiabatic condition, balancing heat loss from the outside of the vessel insulation with heat input from the vessel band heaters. A transient was then initiated where the immersion heater was brought to 100% duty cycle (38 kWe), creating thermally stratified hot and cold pools. After a period of 30 minutes the immersion heater was turned off and the thermally stratified volumes returned to their isothermal condition over a period of 30 minutes. This testing was used for validation data to tune systems code and was used to determine required upgrades needed in the primary system cold pool component insulation, as will be discussed. A plot showing the hot and cold pool thermocouple response for one Test #1 from Table 1 has been included in Figure 5. As can be seen, the hot and cold pools become stratified quickly after turning on the core immersion heater and return to their isothermal condition when the core is turned off.

Table 1: A selection of tests from the primary system experimental campaign. These tests created a stratified condition in the hot and cold pools to provide experimental data for systems code and CFD validation. *Adiabatic condition on outside of vessel set by determining steady state power input required to maintain isothermal sodium in METL vessel without core heater on.

Test #	Outlet Window (6=top)	Mean Start Temperature		Pump Speed [RPM]	Flow Rate [GPM]	Vessel Heaters	Immersion Heater
		Cold Pool [°C]	Hot Pool [°C]				
1	6	202.40	202.50	950	12.5	Off	100%
2	6	202.22	202.35	710	8.6	Off	100%
3	6	201.98	202.10	160	1	Off	100%
4	1	200.99	201.23	950	12.5	Off	100%
5	1	201.88	201.98	710	8.6	Off	100%
6	1	202.08	202.49	160	1	Off	100%
7	6	202.06	202.19	950	12.5	Adiabatic*	100%
8	6	202.93	203.13	710	8.6	Adiabatic*	100%
9	6	201.99	202.22	160	1	Adiabatic*	100%
10	1	201.41	201.59	950	12.5	Adiabatic*	100%
11	1	201.23	201.52	710	8.6	Adiabatic*	100%
12	1	201.77	201.99	160	1	Adiabatic*	100%

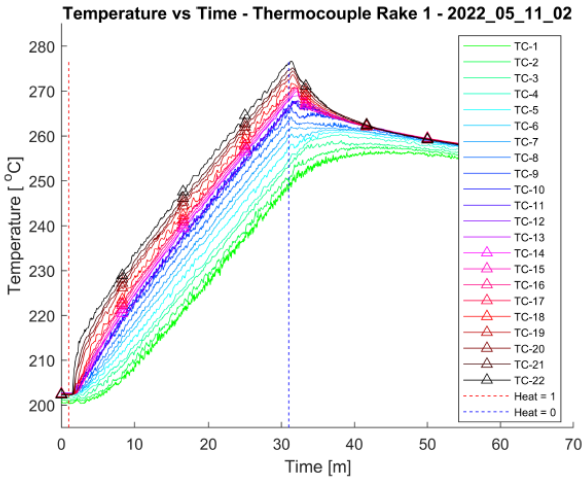

Figure 5: Temperature response during a thermal stratification transient test in THETA. Conditions for test included as Test #1 in Table 1. Thermocouples are part of a single vertical multi-junction probe spanning the cold and hot pools. Thermocouples are numbered in sequential order starting with TC-1 at the bottom of the cold pool. TC-14-22 are in the hot pool and include a triangle marker on the plotted line for clarity. As can be seen a vertical red dotted line indicates the core electrical power being turned on and the blue dotted line indicates the core electrical power being turned off.

2.1.2. Primary Pump Performance Characterization

The maximum permissible pump speed, and corresponding sodium volumetric flowrate at 200 °C, in the primary THETA test article before leakage occurred from the top of the column pipe was determined. As discussed in [2] there is a critical pump operating point where enough fluid escapes the top of the pump case via generated head to be forced over the column pipe surrounding the shaft, Figure 6. This critical operating point was determined in 20 °C deionized water to be at a pump speed of 1,150 RPM with a flowrate of 11.4 GPM. This operating point was determined visually with water, in order to determine this point with sodium a 1/8" K-type ungrounded thermocouple probe was positioned at the top of the column pipe. The probe in the argon gas space will remain at the argon temperature until sodium begins to escape the top of the pipe, where a discreet jump in temperature will be readily apparent.

Figure 6: Photo showing water escaping the top of the column pipe

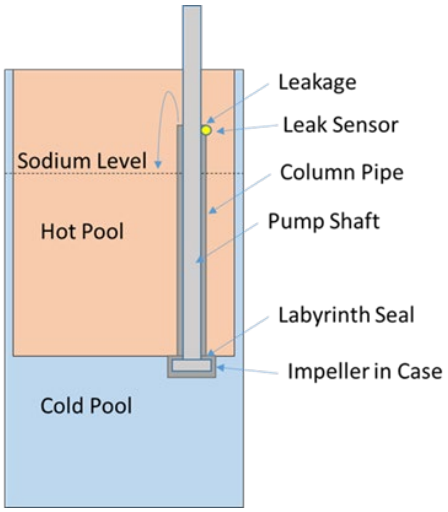

Figure 7: Schematic showing sodium leak path from pump case, through labyrinth seal, and out of the top of the column pipe

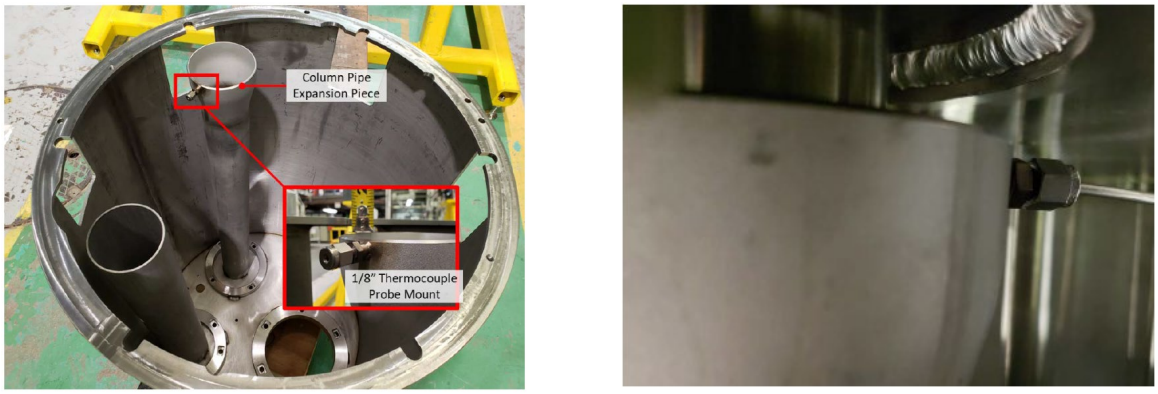

Figure 8: Photos showing the location of the 1/8" ungrounded K-type thermocouple probe located at the top of the column pipe. The photo on the right demonstrates the close proximity of the top of the column pipe to the bottom of the primary THETA flange.

The pump speed was increased from 0-1500 RPM in 100-RPM increments for a period of 20 seconds for each increment. The test described herein was labeled test number 2023-02-07-01. A plot showing the pump speed set point and flowrate as a function of time has been included in Figure 9. As can be seen during the first 10 seconds of the test the flowrate is reduced from around 7.5 GPM to zero GPM, this is because the pump was running for a period of 1 hour before commencing this test to ensure isothermal temperature throughout the system. A plot showing the pump inlet temperature and flowmeter magnet temperature vs time can be found in Figure 10.

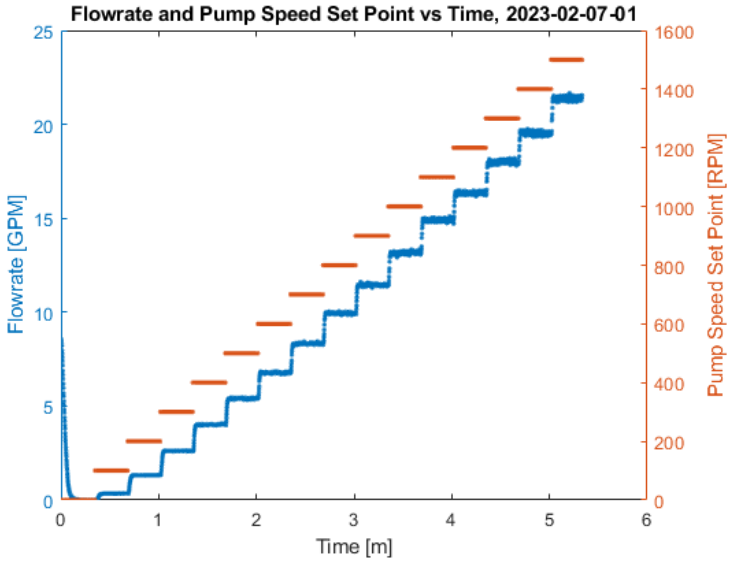

Figure 9: Sodium flowrate and pump speed as a function of time.

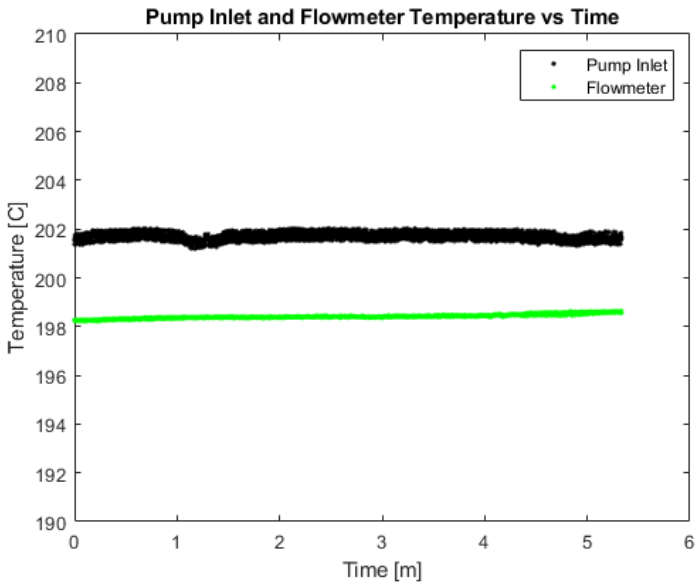

Figure 10: Pump inlet and flowmeter temperature vs time

The overflow thermocouple sensor temperature was plotted alongside the flowrate as a function of time in Figure 11. Figure 12 provides a zoomed in view of the point at which a discrete jump in overflow sensor temperature was witnessed. As can be seen, the jump occurs at flowrates at or above 18 GPM. This indicates that the maximum operating flowrate that can be conservatively maintained without risk of leaking out of the top of the column pipe is 16.5 GPM. This flowrate corresponds to a pump speed of 1200 RPM, representing the maximum pump speed for sodium at approximately 200 °C, Figure 13 and Figure 14.

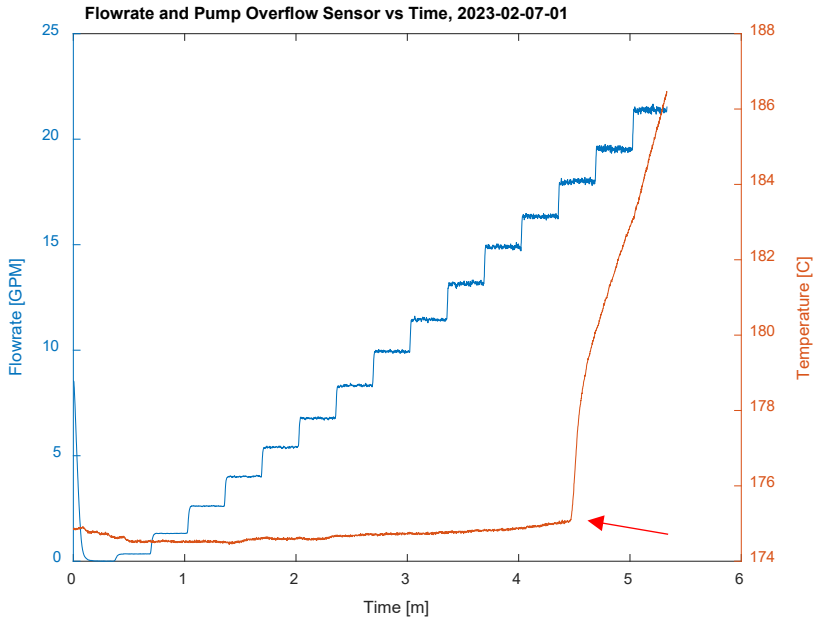

Figure 11: Sodium flowrate and pump overflow sensor temperature vs time. Red arrow pointing to the point at which sodium touches the overflow sensor temperature, indicating when sodium is leaking out of the column pipe surrounding the pump shaft.

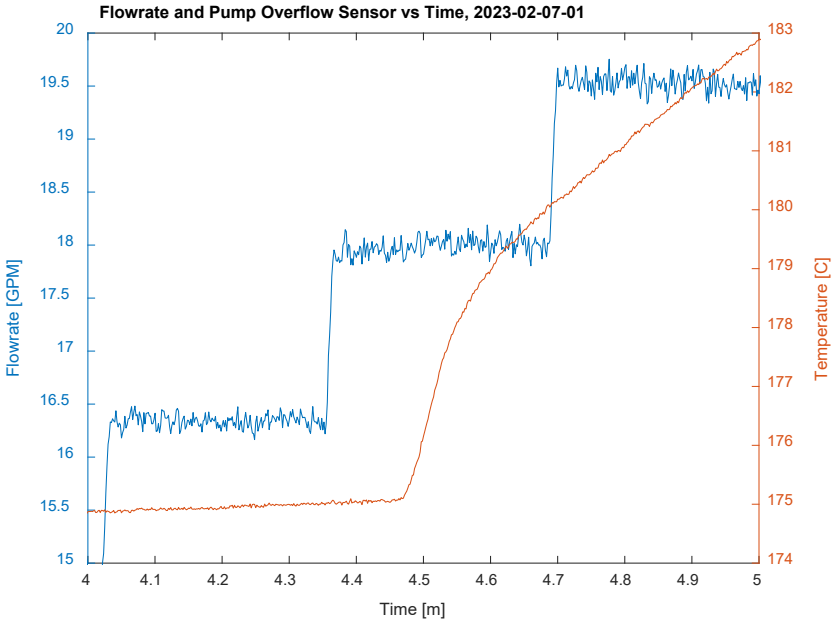

Figure 12: Sodium flowrate and pump overflow sensor temperature vs time

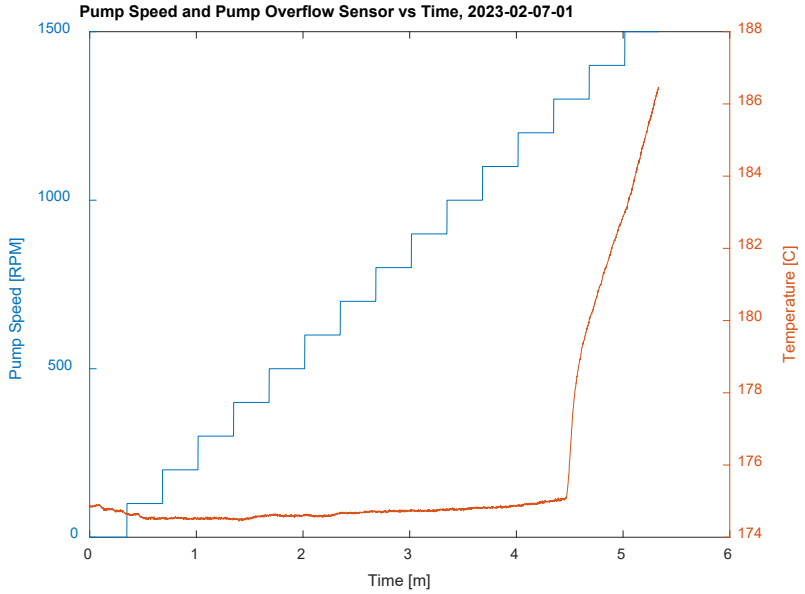

Figure 13: Pump speed set point and pump overflow sensor temperature vs time

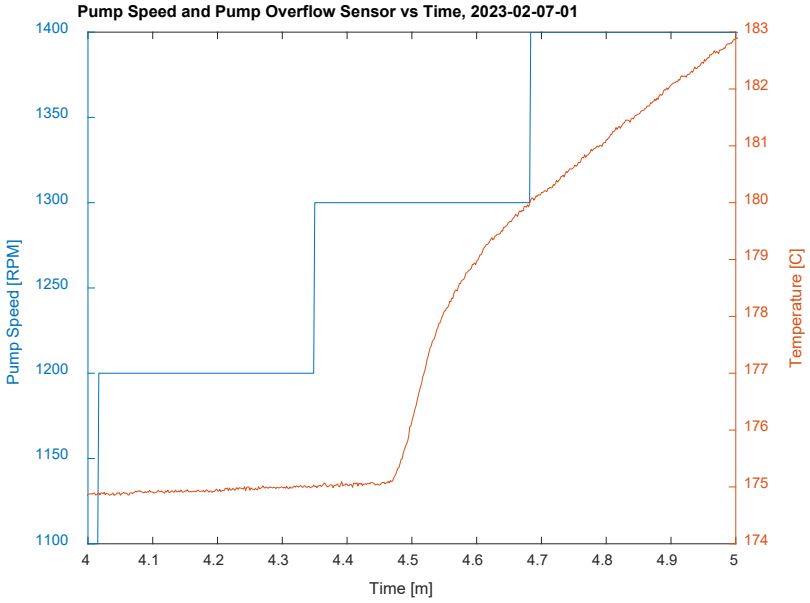

Figure 14: Pump speed set point and pump overflow sensor temperature vs time

The flowmeter data from the test described above, 2023-02-07-01, was compared to an identical test performed 9 months prior, 2022-05-23-01 [3]. As can be seen in Figure 15 the flowrates as a function of time were both plotted showing nearly identical pump and flowmeter performance indicating no loss or change in operation of the pump or flowmeter.

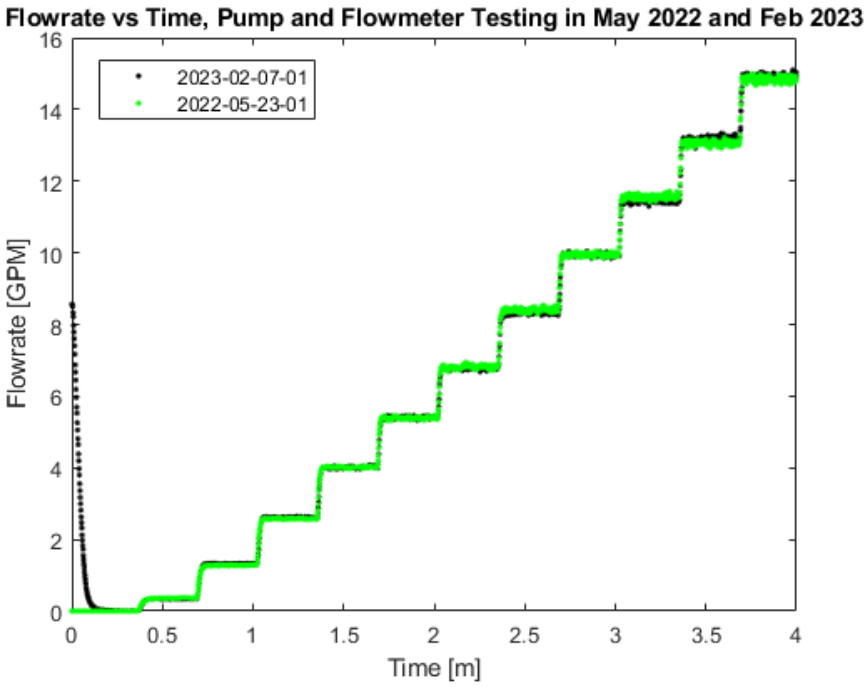

Figure 15: Flowrate vs time for identical pump speed transient demonstrating sustained performance of pump and flowmeter over a period of ~9 months. Average sodium pump inlet temperature for 2023 test: 201.7 C with a standard deviation of 0.15 C. Average sodium pump inlet temperature for 2022 test: 203.1 C with a standard deviation of 0.20 C.

In conclusion, the maximum pump speed and THETA primary system flowrate was determined to be approximately 16.5 GPM and 1200 RPM, respectively, before leakage occurred out of the pump column pipe surrounding the shaft. During testing, the pump was brought to a speed of 1500 RPM yielding a sodium flowrate of 20.3 GPM. Note that this testing was performed at a single sodium temperature of 200 °C – leakage may occur at a different pump speed at different sodium temperatures due to density/viscosity variation; however, given the overflow sensor is always online during testing- the leak point may be determined in real-time for a particular set of test parameters.

In conclusion, if a particular test requires zero leakage from the top of the pump column pipe the pump speed and flowrate should be limited to approximately 1200 RPM and 16.5 GPM. Pending the development of a high-speed bearing to support the end of the shaft to reduce radial oscillatory deflections at speed to

facilitate the use of a more effective case seal this leakage will occur. Note that this leakage is only a problem when performing careful thermal hydraulic experiments with THETA – if mass transfer from the pump column pipe into the hot pool is not a problem, then the pump may be operated above 1200 RPM. For reference, the pump motor possesses a maximum speed of 3520 RPM.

2.2. Primary System Computational Fluid Dynamics and Systems Code Development

Work continues to develop a systems code model of THETA in SAM and SAS4A/SASSYS-1. THETA primary system testing data was used to validate a computational fluid dynamics model in ANSYS Fluent [4].

2.3. Primary System Removal and Sodium Cleaning

2.3.1. Testing of 28" Flexicask

The METL 28" Flexicask system was assembled and tested for the first time in order to facilitate the removal of THETA. Figure 16 shows the Flexicask bottom gate, top gate, glovebag and top mounting plate being tested on a 28" flange. The glovebag was pressurized with an air compressor to just above atmospheric pressure to ensure all the sealing surfaces were gas tight. A custom plate was made to interface the Flexicask top mounting ring with a load spreader with lifting points appropriate for the THETA primary flange's two lift points, Figure 17.

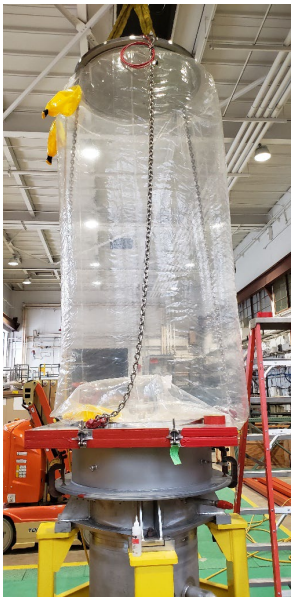

Figure 16: 28" Flexicask being tested with air to ensure glovebag and gate valve assembly gaskets are all working correctly

Figure 17: Custom top mounting plate was designed and installed into Flexicask assembly to accommodate a load spreader with the correct dimensions and weight rating for the THETA test article.

2.3.2. THETA Primary System Removal from METL Vessel with Flexicask

In order to install upgraded insulation and instrumentation to the THETA primary system, the test article was removed and transported to the carbonation system for cleaning. This was accomplished with the use of the METL 28" Flexicask system. Note this was the first time employing the 28" Flexicask system; previous experience utilizing the 18" Flexicask system to remove and replace the Gear Test Assembly from METL was beneficial as the operators were familiar with the general order of operations.

Figure 18 provides pictures detailing the overall steps in using the 28" Flexicask to remove THETA. As can be seen in Figure 18.a the motor on the primary pump was removed to reduce the overall height of the primary system and to move the center of gravity of the system further inward. Bottom gates were installed on both the THETA vessel and the carbonation system, Figure 18.a and Figure 18.b. Both of these vessels were then inerted with argon. The Flexicask top gate, glovebag, and mounting plate assembly with spreader bar were then rigged to the top of the THETA primary system, Figure 18.c. At this point an argon gas line was attached to the bottom gate of the Flexicask and a port on the top of the Flexicask mount plate was opened to inert the glovebag, pushing air out of the top of the system with the heavier-than-air argon gas.

The THETA system was then lifted from the vessel and the bottom gate was inserted into the bottom gate assembly to reduce oxygen ingress into the METL vessel, Figure 18.d. When the bottom of the THETA test article cleared the top gate assembly, the top gate was inserted and the two gate assemblies could be separated, Figure 18.e. The crane was then used to transport THETA, under inert cover gas via the Flexicask, to the carbonation system vessel, Figure 18.f. The top and bottom gate assemblies were attached together at the carbonation system vessel and their respective gates were removed, Figure 18.g. THETA could then be lowered into the carbonation system until the THETA primary flange mated with the carbonation system flange, Figure 18.h..

A blank flange was then picked up with the Flexicask system and the Flexicask top gate assembly was reattached to the bottom gate assembly as in Figure 18.i. The glovebag could then be inerted with argon before removing the bottom gate to facilitate lowering the blank 28" flange onto the METL vessel to seal the system. Finally, the blank flange was bolted to the vessel to maintain an inert environment while THETA was being upgraded, Figure 18.j.

(a)

(b)

(c)

(d)

(e)

(f)

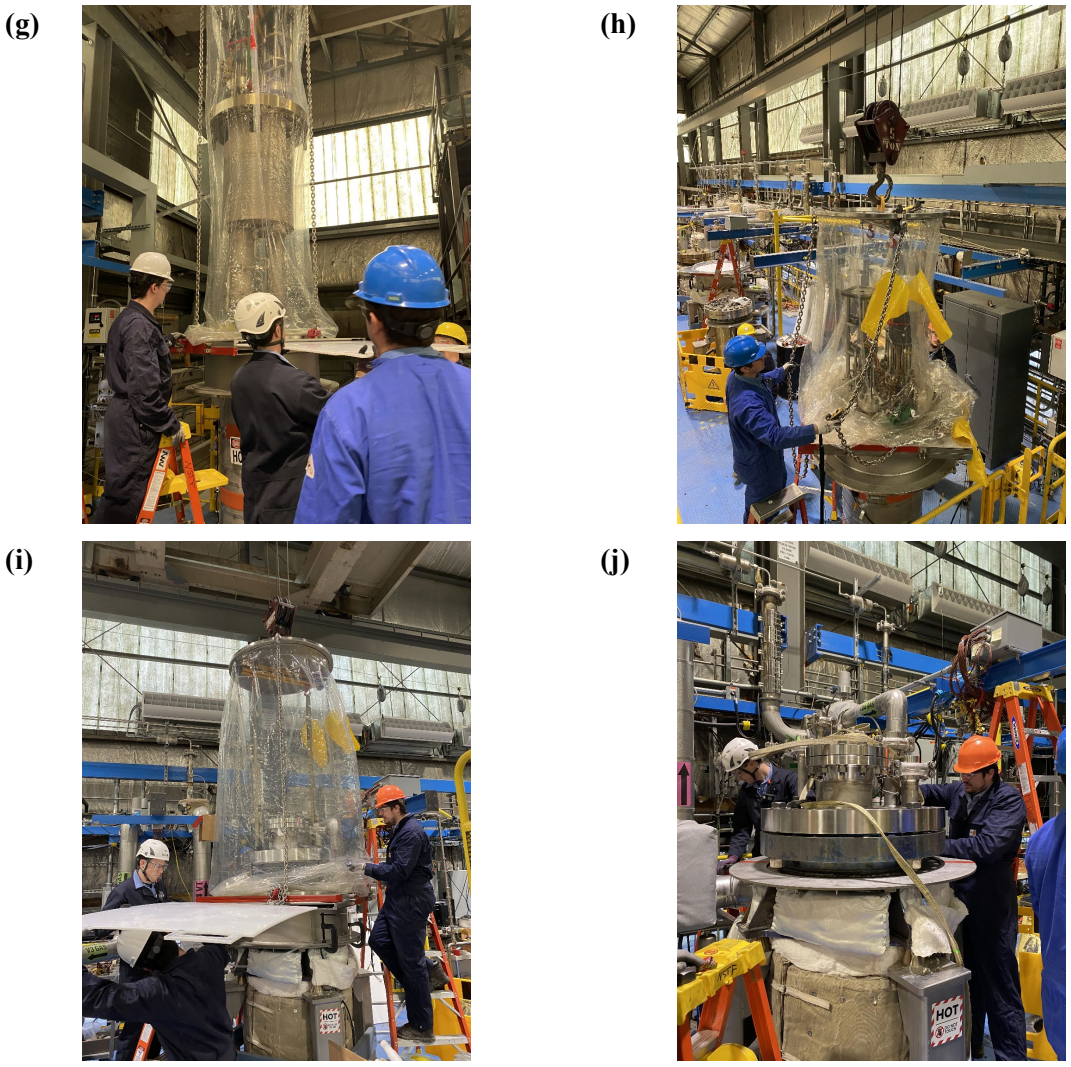

Figure 18: Operation of the 28" Flexicask system to remove THETA for carbonation. Steps have been described in detail in the text.

2.3.3. Carbonation

Following the removal of THETA with the Flexicask system, the test article was immediately inserted into the METL carbonation system vessel. The carbonation system employs moist CO_2 to react with solid sodium residue on the test article surfaces to slowly produce sodium carbonate/bicarbonate and hydrogen gas. The hydrogen gas is monitored and safely removed from the system. More information on the METL carbonation system, including photographs, reaction equations and P&IDs please see [5].

THETA was reacted in the carbonation system for a period of 1 week with the CO_2 –water sparging tank at 80-85 °C. The flowrate of the moist CO_2 was varied between 5-10 SLPM. A photo of the current carbonation control system is included in Figure 19 where the sparging tank and human-machine-interface can be seen. Photos of THETA after removal from the carbonation system can be found in Figure 20 to Figure 26. As can be seen in Figure 21, large droplets of sodium that were frozen to the bottom of the inner

vessel were sufficiently wetted to the surface that they were fixed in place during carbonation and formed sodium carbonate surface ‘stalactites’ with pure sodium cores. All the sodium that resided on horizontal surfaces were reacted as well but left some residual pure sodium beneath the carbonate, Figure 22. The carbonate was chipped off easily into a catch pan with a scraper, Figure 23. Crystalline formations were also observed on some of the carbonate surfaces, Figure 24. A large amount of sodium resided in the bottom of the hot pool but was sufficiently exposed to fully react with the carbonation process with a small amount of solid sodium remaining, as will be discussed in the next section, Figure 25-Figure 26.

Overall, the carbonation process created an inert biproduct that was easy to remove mechanically with scrapers, brushes, and deionized water (being careful to ensure no solid sodium existed beneath the carbonate surface). When the process was applied to large volumes of sodium residing on surfaces with ample room for volumetric expansion and exposure to complete the reaction it is an ideal cleaning technique. However, as will be seen, smaller volumes of trapped sodium, such as in process piping, where the carbonation process biproduct was not able to expand and where trapped volumes of sodium became inaccessible to the reaction, the process was not favorable and lead to further complications.

Figure 19: Photo of the carbonation system showing the control computer, process heater controllers, and CO_2 sparging tank.

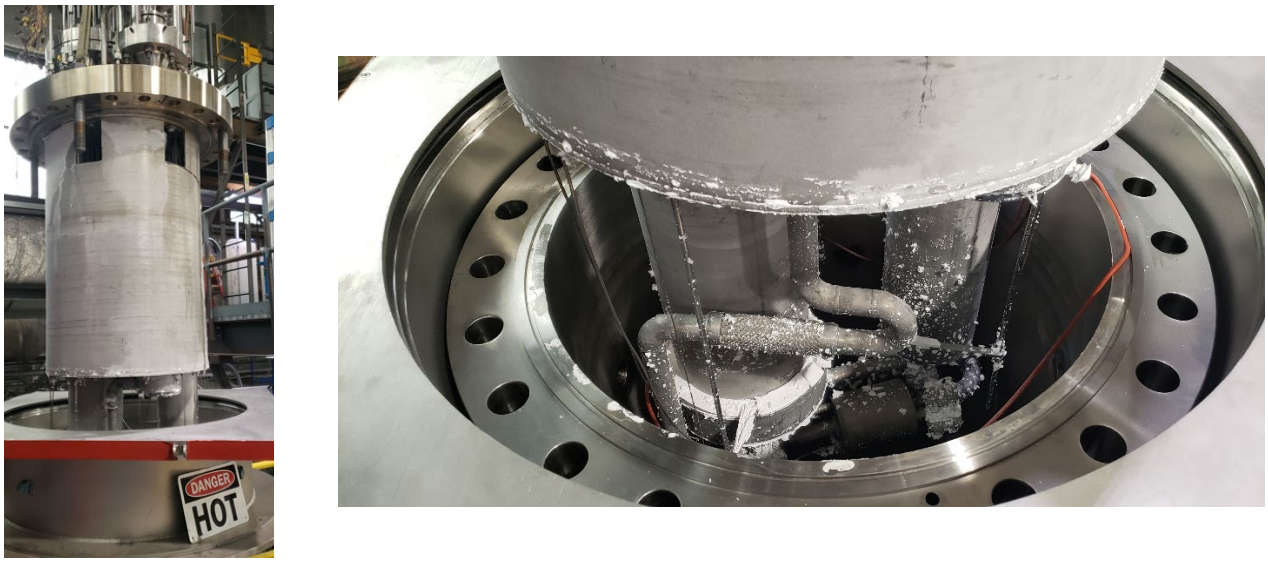

Figure 20: Photo of THETA being hoisted from the carbonation vessel.

Figure 21: Photo of some of the sodium (bi)carbonate residue on the bottom of the hot pool inner vessel as THETA was being hoisted from the carbonation vessel.

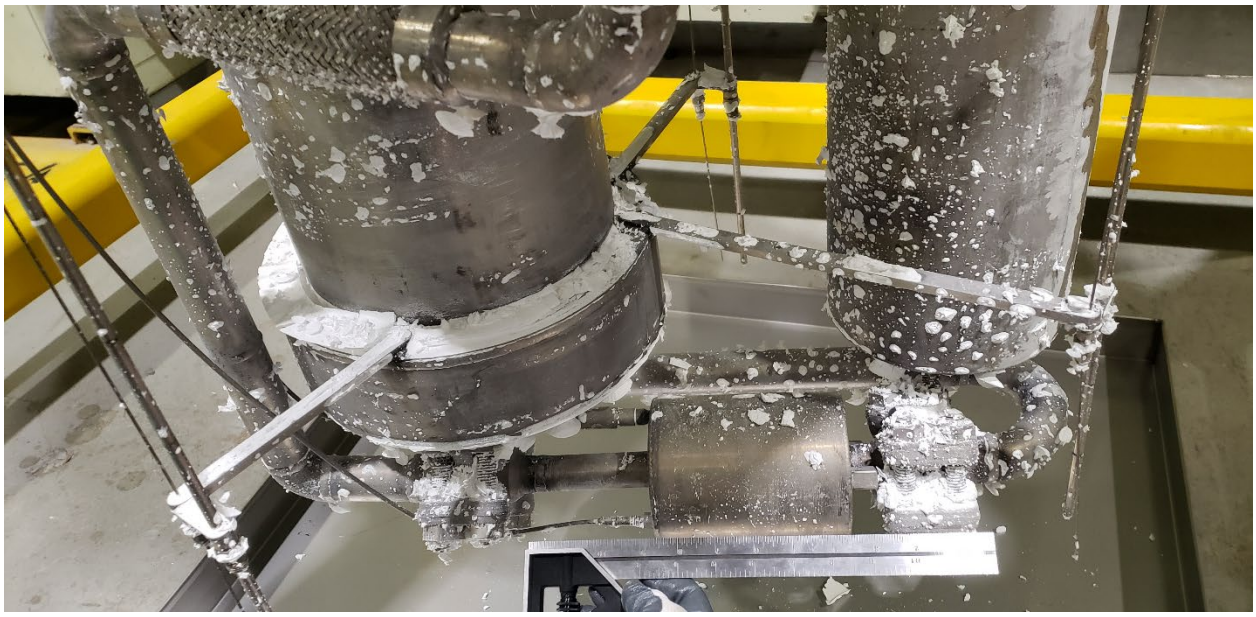

Figure 22: Photo showing sodium (bi) carbonate residue on the lower cold pool ponents.

Figure 23: Photo showing sodium (bi)carbonate residue that was mechanically chipped off of the surfaces into a stainless-steel catch pan with ease. The bi(carbonate) was then processed in the METL burn stall with dry steam, wet steam, then water, all with no detectable chemical reaction.

Figure 24: Photo showing some of the (bi)carbonate reaction product on the underside of the THETA inner vessel, near the outlet of the IHX. As can be seen, some crystallized formations seem to have developed during the carbonation reaction process.

Figure 25: Photo showing the inside of the THETA hot pool inner vessel with the core immersion heater removed. The carbonation process reacted the sodium in this large cavity quite well. The bi(carbonate) was mechanically scraped and a dedicated vacuum was used to remove the biproduct into a plastic bag for sodium decontamination. Small pockets of pure sodium remained under the carbonation product which were cleaned with ethanol then deionized water.

Figure 26: Photo showing a closer view of the carbonation byproduct in the inner vessel.

2.3.4. Primary System Sodium Cleaning

Following the carbonation process, the primary system was mounted to a METL test article support stand to facilitate further deconstruction to remove sodium (bi)carbonate byproduct and any remaining solid sodium. The THETA core was removed from the system and transported to the METL alkali metal burn stall where superheated steam was used to gently remove residual material on the heater elements, Figure 27. Given the high surface area and relatively large pitch of the heater elements the carbonation process was very well suited to reacting all of the solid sodium as there was very little reaction to dry steam and/or deionized water.

The pump case and pump outlet piping were removed, and it was discovered that a significant volume of sodium resided in the lower piping sections highlighted in Figure 28. When installed and at temperature these sections may not have had the appropriate drain angle towards the drain port to discharge sodium when draining the primary system, thus sodium was trapped and solidified in the piping when cooling the experiment to prepare for removal. Figure 29 shows the solid sodium in the piping.

The labyrinth seal on the pump case trapped a small volume of sodium that was mechanically scraped off and treated with ethanol and deionized water, Figure 30. The two 1” Grayloc flanges were disassembled on either side of the submerged flowmeter, Figure 31; the flowmeter could not be removed as the 1/8” mineral insulated thermocouple and induced voltage cables were fed through the bottom of the hot pool inner vessel. Solid sodium had built up around the feedthroughs on the bottom of the inner vessel, prohibiting the cables from being pulled through the bottom. Similarly, the inner vessel lower feedthroughs for the thermocouples and optical fiber capillaries were also frozen with solid sodium, thus the

instrumentation was left in place and the support mounts that were fixed to the core barrel were cut to remove the barrel, Figure 32. The bulk sodium in the flowmeter was removed mechanically with drill bits and lint free wipes, Figure 33.

Figure 27: Core immersion heater being cleaned in the METL burn stall with dry steam, wet steam and deionized water

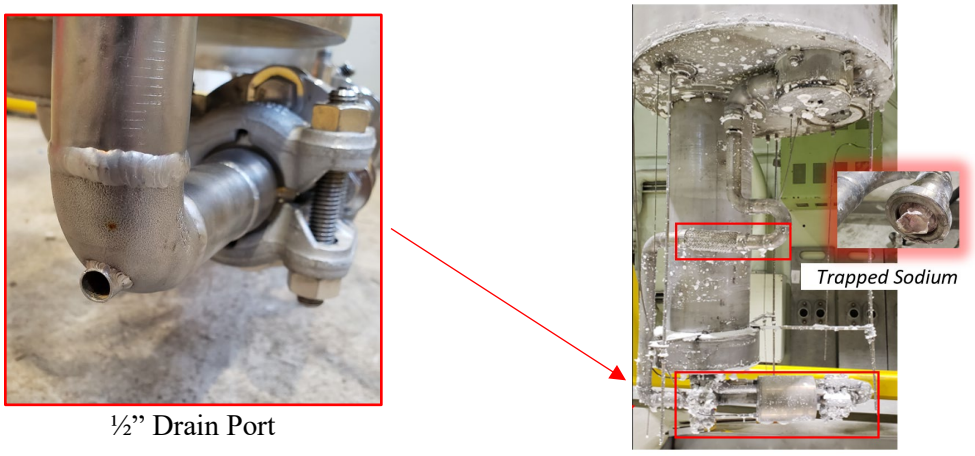

Figure 28: Location of trapped solid sodium in piping section and flowmeter highlighted with red box. Also shown is the drain port at the lowest portion of the primary piping which was supposed to facilitate complete drainage of the system.

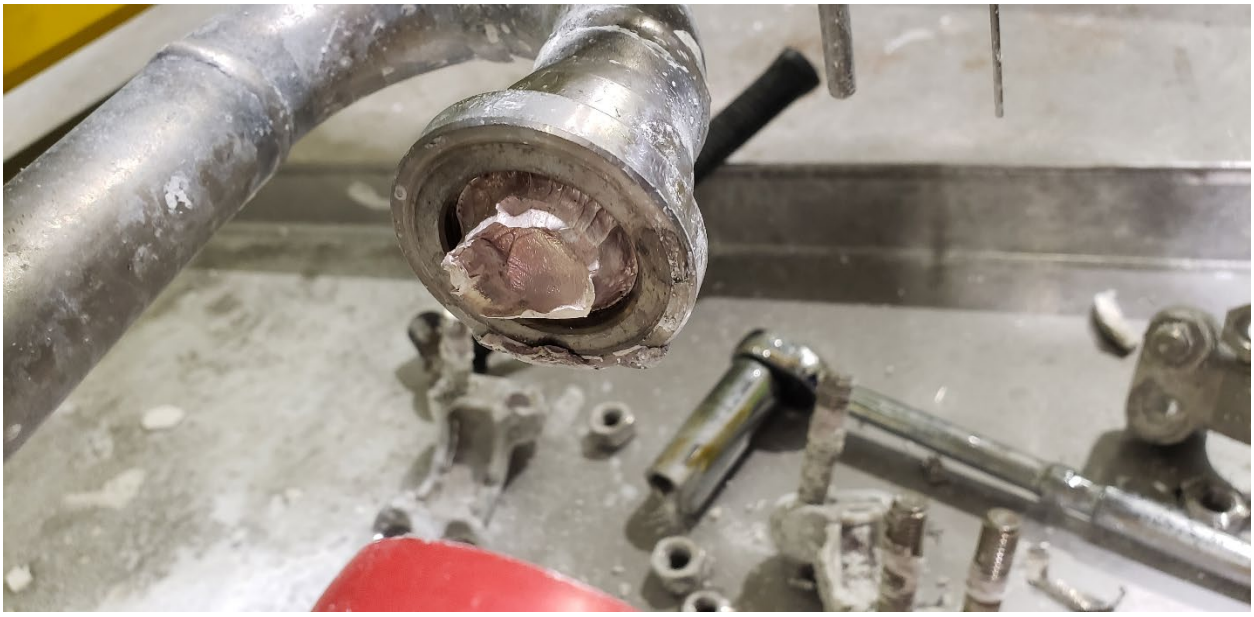

Figure 29: Solid sodium in 1” SCH40 piping after the flowmeter

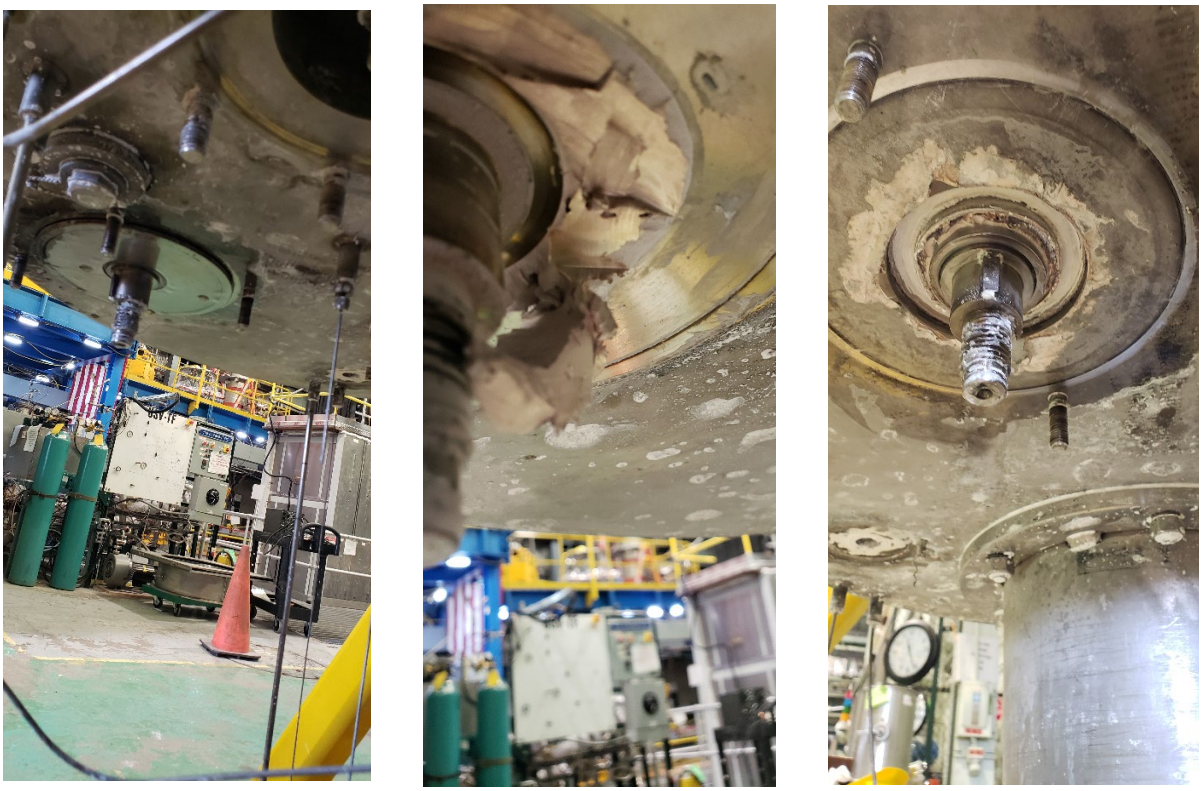

Figure 30: Labyrinth seal with pump shaft protruding, left. Labyrinth bottom plate removed and sodium scraped from the bottom of the vessel, middle. Sodium being cleaned from the shaft to allow for top portion of labyrinth seal to be removed, right.

Figure 31: 1” Grayloc connections removed from either side of flowmeter.

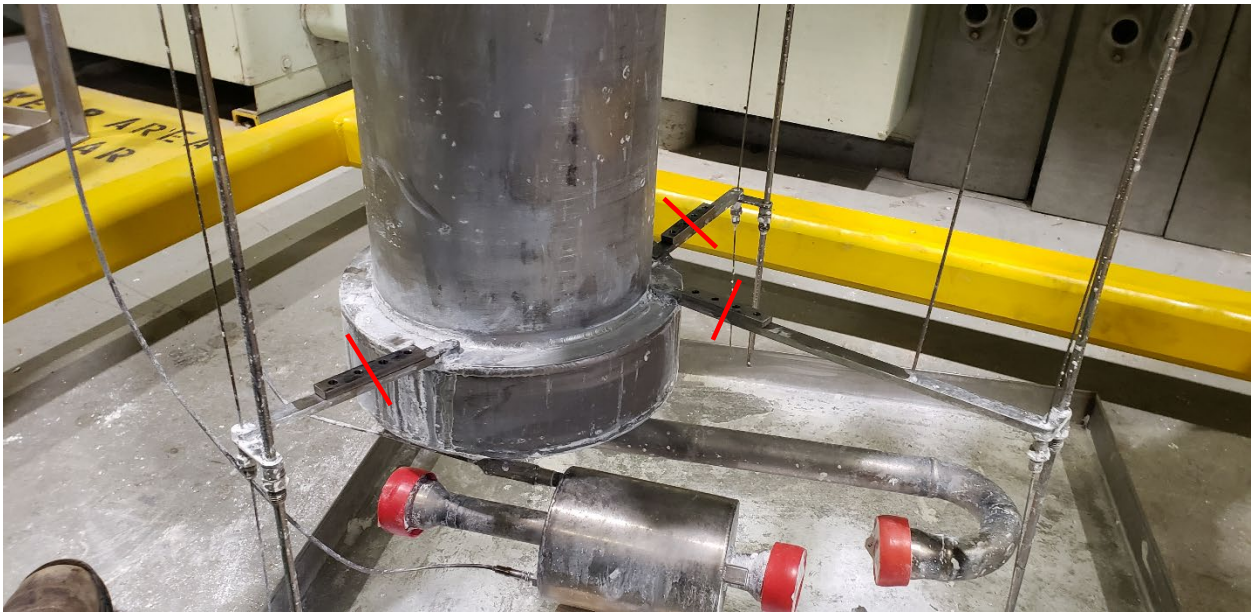

Figure 32: Locations where cuts were made on the instrumentation supports were made to facilitate removal of the core barrel.

Figure 33: Drill bits were used to remove bulk sodium from the flowmeter, top. The drill bits were treated in the burn stall to remove bulk sodium from the flutes, middle. Dry lint free wipes were then used to remove loose surface sodium on the inner walls of the flowmeter, followed by lint free wipes with ethanol, then ethanol diluted with deionized water, and finally deionized water, bottom.

The core barrel, pump case, intermediate heater exchanger outlet and all cold pool piping were transported to the burn stall to remove the relatively large volume of solid sodium, Figure 34. All sections of piping where solid sodium was suspected to reside were heat traced and insulated. The temperature of these sections was brought to 120 °C. A stainless steel bucket was inerted with argon and the liquified

sodium was drained into this vessel, Figure 35. With the bulk of the sodium cleared from the pipe, superheated steam could be used to clear the rest of the residual sodium from the piping inner walls.

The thermal expansion joint on the pump outlet piping was discovered to have been damaged after removal from the carbonation system. It is suspected that the carbonation process, which results in volumetric expansion of the sodium when reacting to sodium (bi)carbonate, damaged the relatively fragile flexible hose in the expansion joint during swelling. A new expansion joint was procured and welded into the system, Figure 36.

Figure 34: Photo showing the THETA cold pool components with trace heaters and insulation installed. Components oriented to facilitate drainage. Catch pan and argon gas line to inert the pan shown under core barrel piping, prepared for sodium melting.

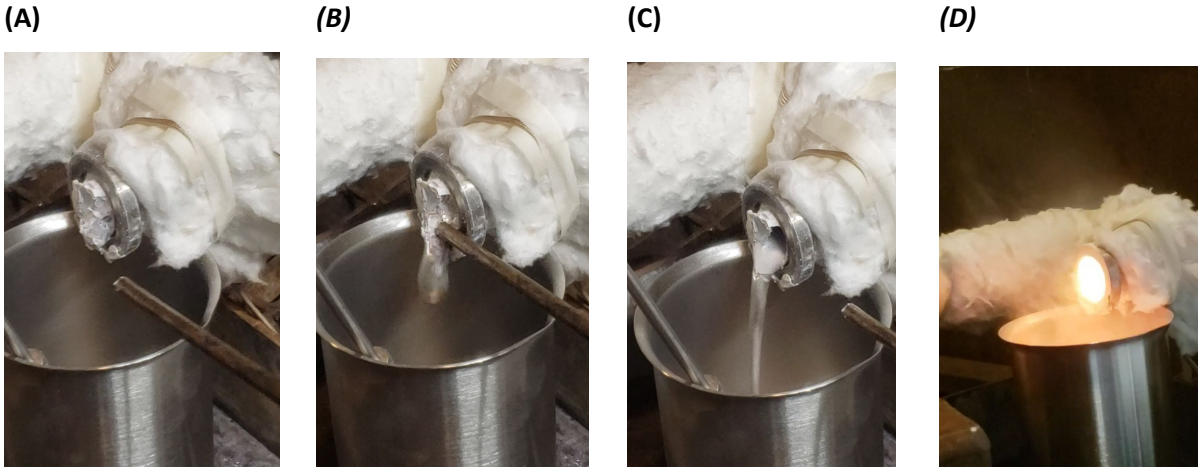

Figure 35: Photo A: trace heating on core barrel piping brought to a set point of 120 °C. B: stainless steel rod used to break solid sodium plug to promote drainage. C: Sodium draining into stainless steel bucket which has an inert argon cover gas. D: after sodium was drained, humid air was able to reach the residual sodium and it began to burn. Trace heaters were shut off and the piping was completely reacted with dry/moist steam followed by deionized water rinse of all components.

Figure 36: Swollen, damaged expansion joint shown as welded into the piping. New expansion joint that was welded in shown immediately below.

2.4. Primary System Upgrades

Following initial thermal stratification testing of THETA, it was determined that the thermal conductivity of the core barrel and intermediate heat exchanger (IHX) outlet was too high to produce useful data for systems code validation. Typically, the thermal hydraulic behavior of reactor components/regions in a systems code are based on correlations or 0 or 1 dimensional body calculations. With high radial heat transfer into the cold pool from the core and IHX outlet, this produces a large amount of thermal stratification and buoyancy driven mixing in the cold pool that the systems code has difficulty resolving. This is because the systems code is designed to represent much larger, full scale reactor geometries than THETA (much higher Peclet numbers). The complete THETA primary system was modeled in ANSYS Fluent for computational fluid dynamics validation purposes- it was seen that when the THETA electrically heater core was set to full duty cycle (38 kWe) and a sodium flow rate of 3.8 L/min the heat transferred directly to the cold pool through the barrel wall was nearly 16 kWt [4]. Thus, it was determined that the core barrel and IHX outlet required great thermal insulation to reduce the heat transfer to the cold pool.

2.4.1. Core Barrel Insulation

The THETA core barrel was insulated with the use of a 'clamshell' sheet metal structure that wrapped around the existing core. This structure provided a 0.44" thick annular region of vacuum or gas space around the core, Figure 37-Figure 38. A thermal resistance network, considering conductive and radiative heat transfer, was used to assess the improvement in radial thermal resistance of the core, Figure 38. It was determined the core insulator provides a ~67x greater thermal resistance.

Given the improvement in thermal resistance and the sudden thermal transients the insulator may undergo as a result of insulating a high watt density immersion heater in conductive sodium, a thermal stress analysis was performed to ensure the design was robust enough. The insulator was fabricated with 16-gauge Inconel 718. Figure 39 provides the temperature boundary conditions and calculated equivalent (von Mises) stress of the ANSYS finite element analysis model. Notice a 100 °C differential in temperature was set across the insulator inner/outer diameter. This resulted in a maximum equivalent stress of 0.6 GPa. The yield strength as a function of temperature was provided on the manufacturer's (ATI Specialty Rolled Products) certificate of test and is included in Figure 40; the yield strength of heat-treated Inconel 718 at 400 °C is 0.9 GPa. The heat treatment schedule recommended by the Inconel supplier that was used after the weldment was fabricated can be found in Table 2.

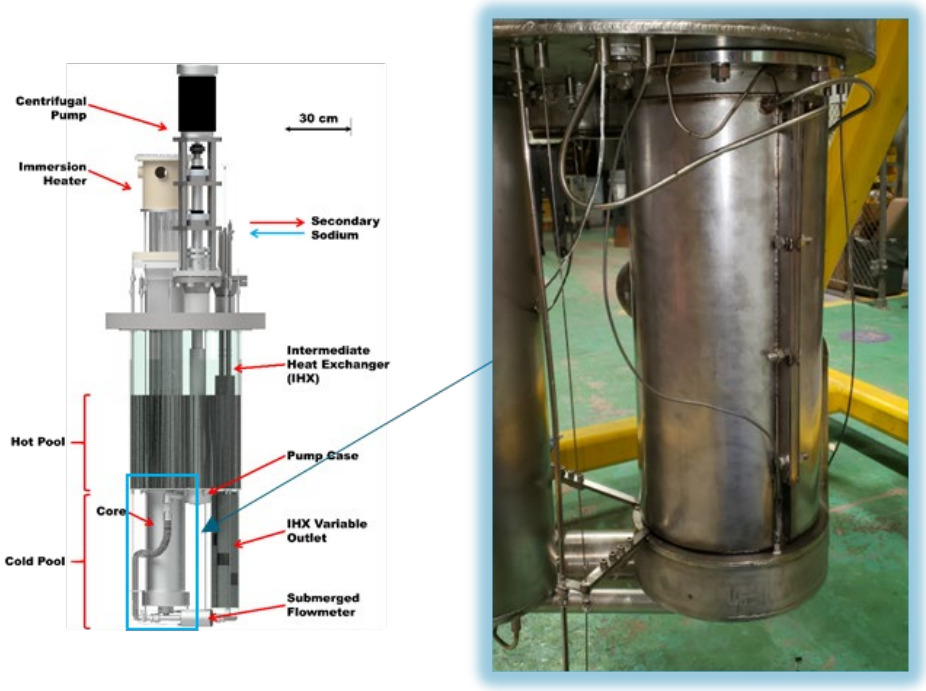

Figure 37: Photo of core insulator with location of component highlighted in primary system drawing

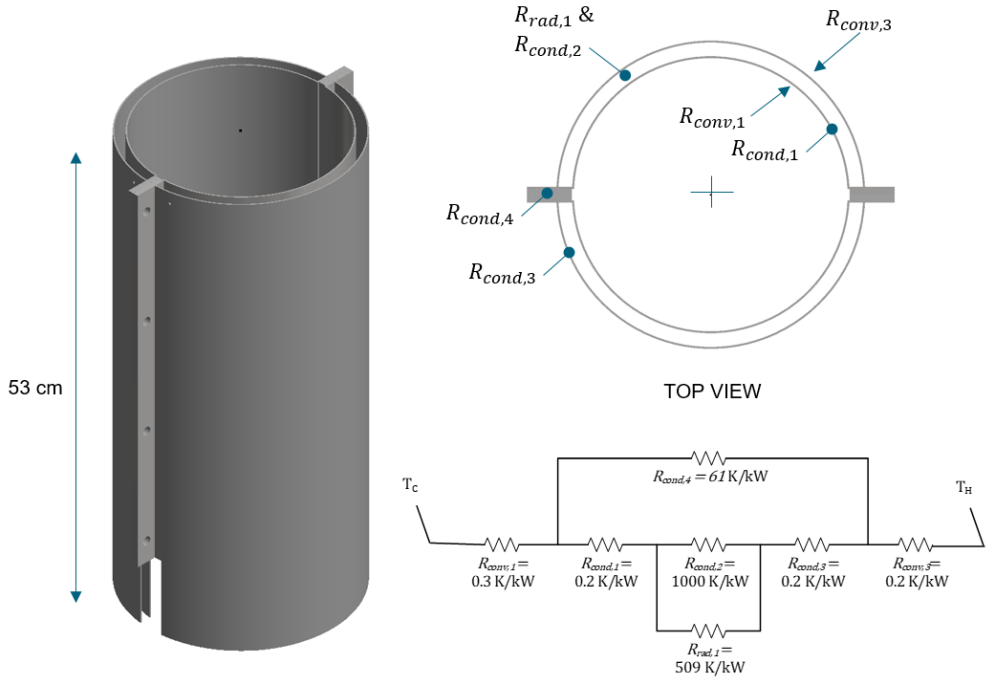

Figure 38: Schematic showing the core insulator as well as the resistance diagram used to determine its effectiveness

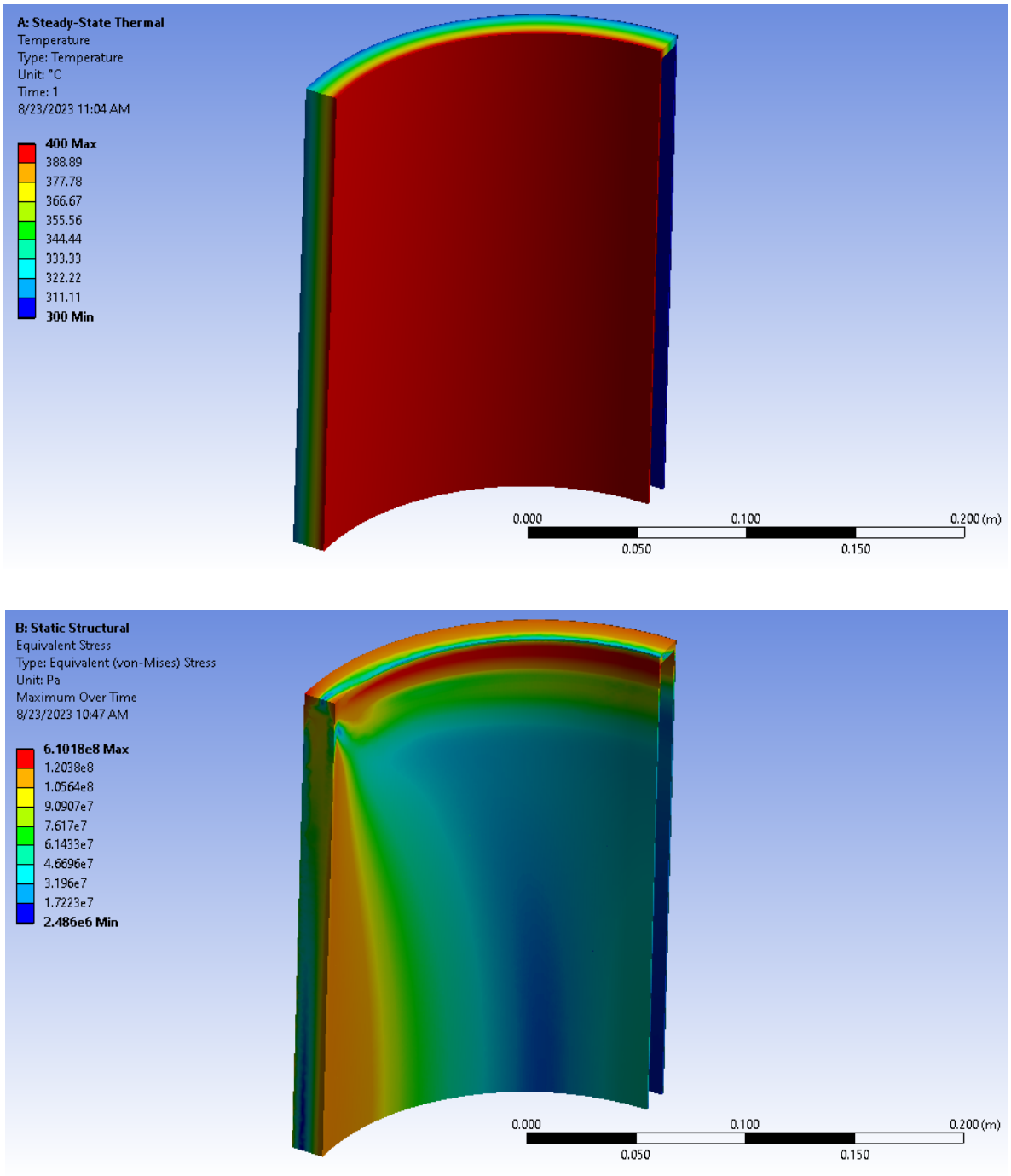

Figure 39: ANSYS finite element analysis model. Model took advantage of axial and radial symmetry to split the geometry into ½ length and 1 quadrant. Temperature boundary condition employed, top. Equivalent (von-Mises) stress calculated, bottom.

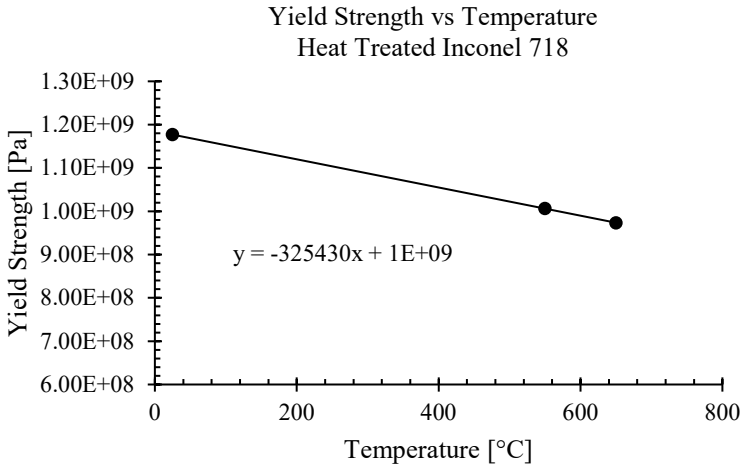

Figure 40: Yield strength of heat-treated Inconel 718 as a function of temperature. Heat treatment schedule (Table 2) and yield strength supplied by ATI Specialty Rolled Products

Table 2: Heat treatment schedule for THETA core insulator 16-gauge Inconel 718 insulator weldment

Step	Process
1	Heat to 1325 +/- 15 °F. Hold at heat for 8 +/- 0.5 hours under vacuum or argon atmosphere
2	Furnace cool to 1150 +/- 15 °F IN 2+0.1/-0 hours
3	Hold at 1150 +/- 15 °F for 8+0.5/-0 hours under vacuum or argon atmosphere
4	Air cool to room temperature

A 1/8” multijunction thermocouple probe with a pitch of 2.375” was spot welded to the core barrel, fitting between the insulator and the core in a channel near where the two clamshell flanges meet, to assess heat transfer performance, Figure 41. Also notice in Figure 41 there are two ¼” stainless steel tubes that are welded to the gas space and are fed out of the top of the primary flange to facilitate maintenance of the vacuum/gas space in situ.

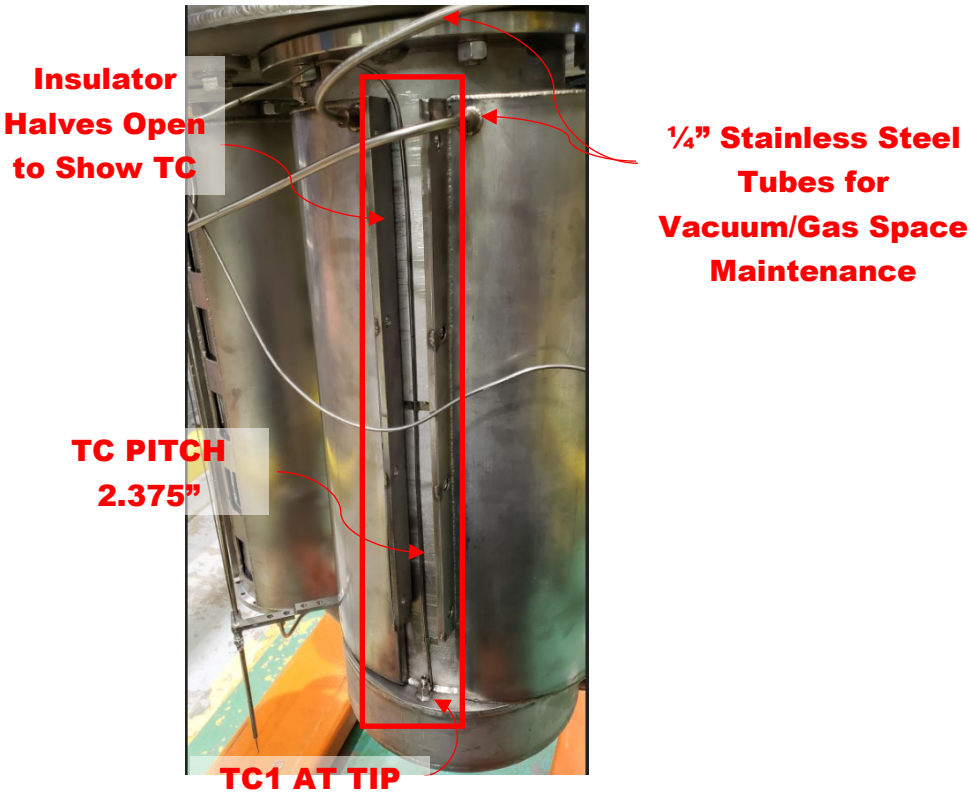

Figure 41: 1/8" diameter, ungrounded K-type multijunction thermocouple probe installed between core and insulator before bolting two clamshells together. A narrow channel was provided near the flange region of the insulator to accommodate the probe. Also highlighted are the two ¼" stainless steel tubes for vacuum/gas space maintenance in situ.

2.4.2. Intermediate Heat Exchanger Outlet Insulation

Similar to the addition of core insulation, an annular region of gas/vacuum space was created around the circumference of the IHX outlet, Figure 42. Figure 43 provides a schematic of the additional insulation as well as a comparison in the resistance network between uninsulated and insulated components. The outlet insulator provides 5.4x more radial thermal resistance (81% reduction in radial thermal conductivity) when considering both conductive and radiative heat transfer. The IHX outlet insulator was constructed with 14-gauge 300 series stainless steel.

The IHX outlet also possessed a ¼" stainless steel tube that allowed the operator to maintain the vacuum/gas space of the insulator while the THETA primary system was installed in METL and filled with sodium. Figure 44 provides a diagram of the vacuum/gas maintenance lines as well as a picture of the insulators as a 34 millitorr vacuum was pulled on their gas spaces and a mass spectrometer leak detection was used to ensure a helium leak rate of <=1E-8 atm-cc/sec.

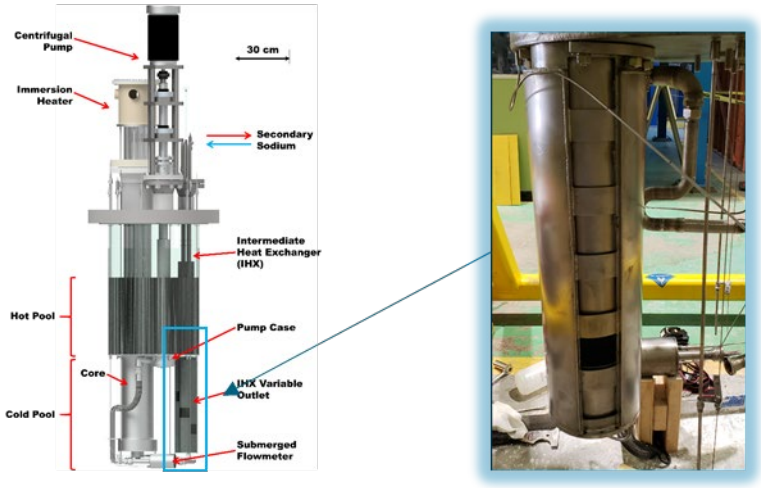

Figure 42: Photo of IHX outlet insulator with location of component highlighted on primary system drawing

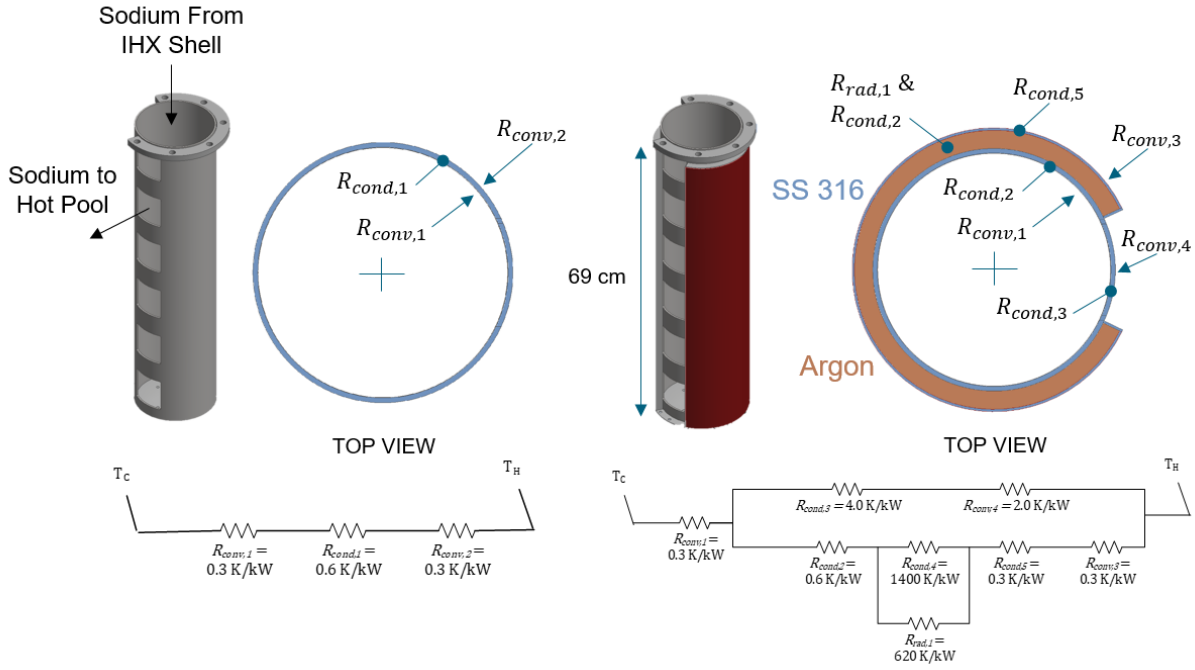

Figure 43: Schematic showing the resistance networks of the uninsulated (left) and insulated (right) IHX outlet barrels.

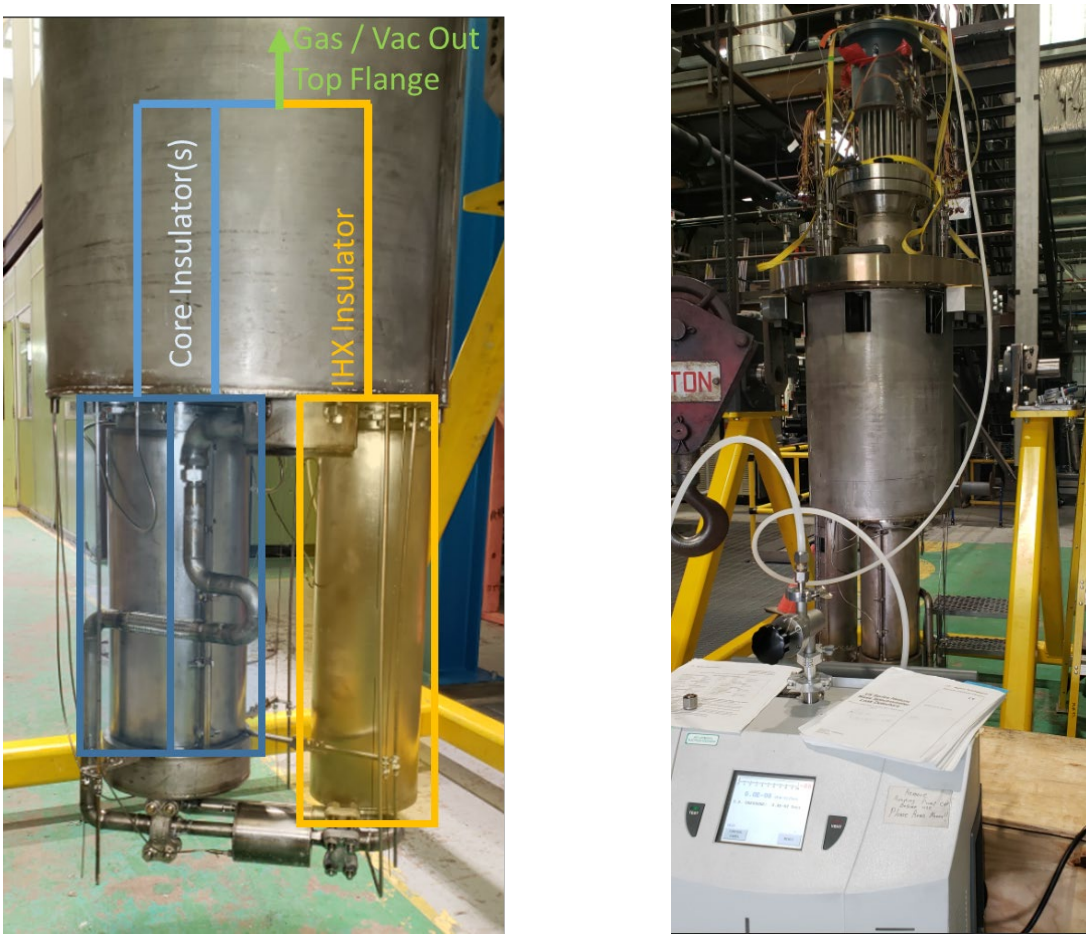

Figure 44: Diagram showing hookup for vacuum/gas maintenance lines, left, and the mass spec lead detection being performed on the two insulators, right.

2.4.3. Final Assembly of Primary System

Following the cleaning of all residual sodium on the primary system, all of the system components and instruments were reinstalled, Figure 45-Figure 47. As can be seen in Figure 46, fastener brackets were fabricated to reattach the instrumentation mounts, that were cut in Figure 32, that rigidly fix the thermocouple rakes and optical fiber capillaries near the bottom of the experiment. Figure 47 shows a picture of a fresh secondary system ¾" outer diameter dip tube that was installed (previous tube was plugged with byproduct during carbonation) as well as a view of the clean inner vessel bottom. Figure 48 illustrates the process of reassembling and realigning the primary pump shaft.

Figure 45: A photo showing the reassembled THETA cold pool components including the upgraded insulation and new thermal expansion piece that was replaced as a result of damage during carbonation volumetric expansion

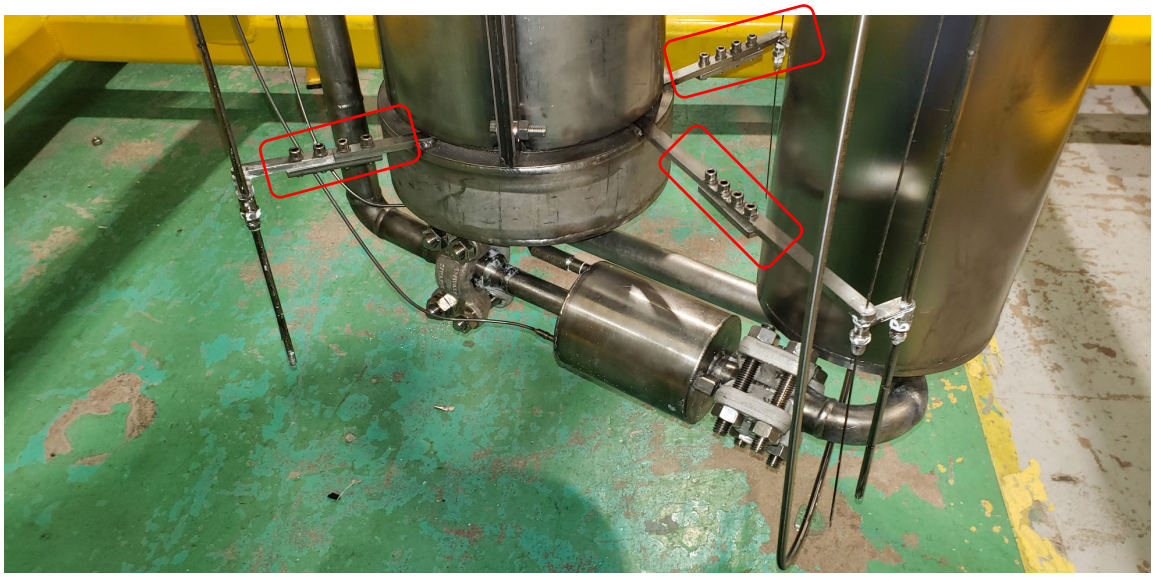

Figure 46: A photo showing the reassembled cold pool components with brackets highlighted that were fabricated to remount the instrumentation fixtures after being cut to facilitate removal of the core for cleaning.

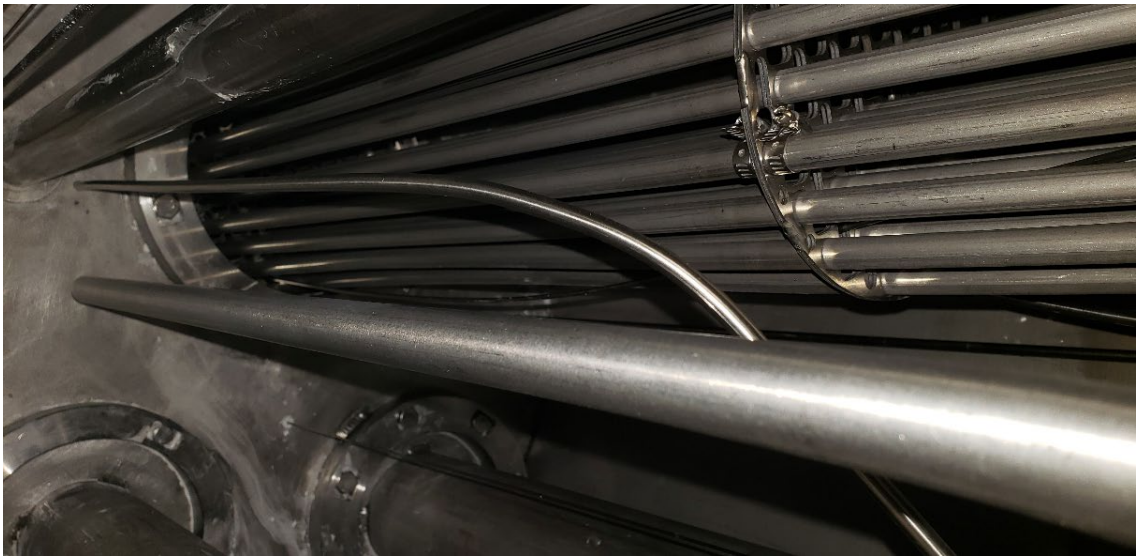

Figure 47: A photo showing the inside of the hot pool with ¾" secondary system dip tube, immersion heater, and instrumentation shown.

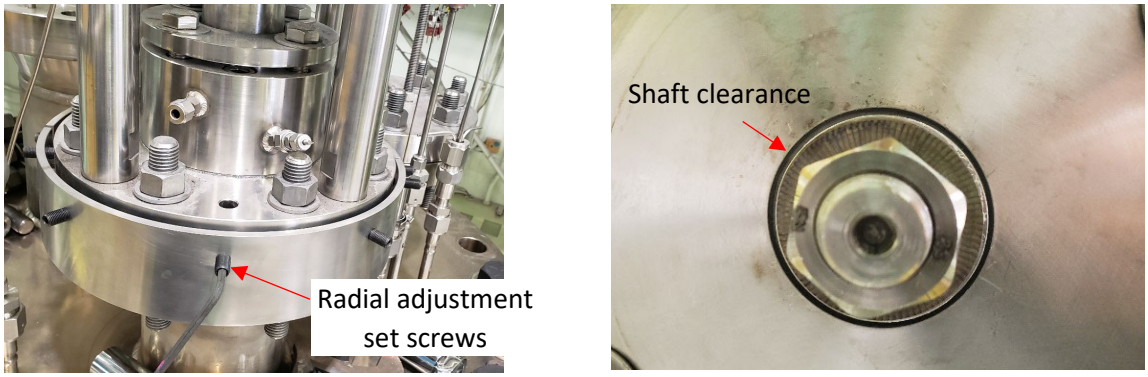

Figure 48: Alignment of THETA primary system pump shaft. Alignment set screws on the top pump flange were adjusted, left, to ensure 0.005" runout in pump shaft did not interfere with labyrinth seal in pump case. A view looking up at the shaft with the impeller removed to show the pump shaft clearance through the labyrinth seal can be seen on right.

2.5. THETA Reinstallation into METL Vessel with Flexicask

With the THETA primary system reassembled, the Flexicask was used to insert the test article back into METL test vessel #4. As can be seen in Figure 49, the process was similar to the removal of THETA. The first step was to install the complete Flexicask system (top/bottom gate valve assembly, glovebag, top mounting plate) onto the vessel, Figure 49.a. Then, the top mounting plate was rigged to the blank flange that was installed on the vessel. The glovebag space was inerted by passing argon gas through the bottom gate valve assembly gas fitting, letting the argon push air out of the top relief fitting on the top mounting plate. Then, the blank flange was lifted from METL vessel #4 and the bottom gate valve was installed to allow the top gate to be detached and the blank flange moved to be placed on a surface that will protect the flange's finely polished sealing surface, Figure 49.b.

The upper assembly of the Flexicask system was then placed over the THETA primary system, with the upper gate valve assembly resting securely on the test article stand, Figure 49.c-d. With the upper gate valve assembly resting on the test stand, the primary system was rigged to the top plate spreader bar and hoisted upwards until the bottom of THETA cleared the top gate valve assembly, Figure 49.e.

THETA was then transported to METL test vessel 4 where the top and bottom gate valves assemblies were mated, Figure 49.f. The glovebag could then be inerted with argon before pulling the bottom gate valve and lowering THETA into METL test vessel 4, Figure 49.g. With THETA installed the Flexicask system could be removed, Figure 49.h.

(a)

(b)

(c)

(d)

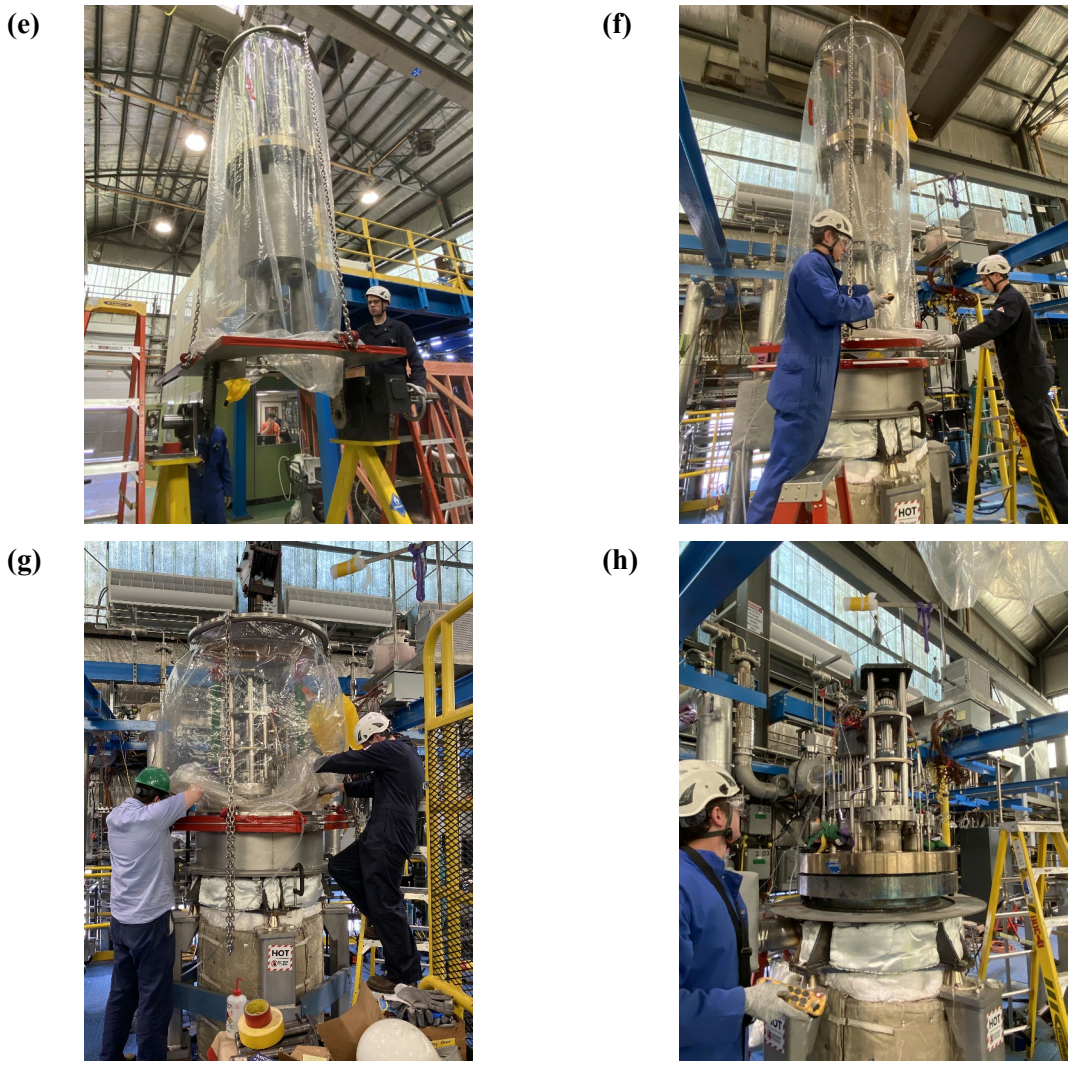

Figure 49: Operation of the 28" Flexicask system to replace THETA back into METL test vessel #4 after cleaning and reassembly. Steps have been described in detail in the text.

2.6. Primary System Testing with Insulated Cold Pool Components

2.6.1. Pump and Flowmeter Performance

Following a refill of the primary system with sodium, the pump and flowmeter performance was assessed by completing the same pump speed transient as described in Figure 9. The flowmeter demonstrated a marked reduction in measurement- as seen in Figure 50 where the flowrate vs pump speed was plotted for data before removal and after reinstallation of the primary system. The primary system flowmeter possesses the same signal to noise ratio as before THETA removal, the instrument was not physically damaged, and the Curie point of the SmCo magnets, 550 °C [6], was never reached. The pump was not damaged and was reassembled properly, the maximum pump speed before sodium leakage out of the top of the column pipe was shown to be 1200 RPM, Figure 51, this was the same as before removing THETA for cleaning as shown in Figure 14.

Currently it is suspected that poor wetting of the flowmeter is to blame for the marked reduction in measured flowrate. It is known that poor wetting can result after a system has been opened to atmosphere and the pipe cleanliness is compromised [7]. As described before, the flowmeter could not be removed from the primary vessel assembly to be cleaned with dry steam and deionized water flush. Sodium was pushed through the flowmeter for a period of at least 15 hours at temperatures ranging from 200-300 °C without a drastic improvement in signal performance. A dedicated wetting campaign will be pursued next fiscal year where sodium from METL vessel #4 will be actively cold trapped to 2 wppm oxide concentration while sodium is pushed through the flowmeter with the primary pump at a temperature of at least 300 °C for an extended period of time. The flowmeter will be determined to be fully rewetted when the generated flowrate from the transient described in Figure 9 matches the data from pre-removal conditions.

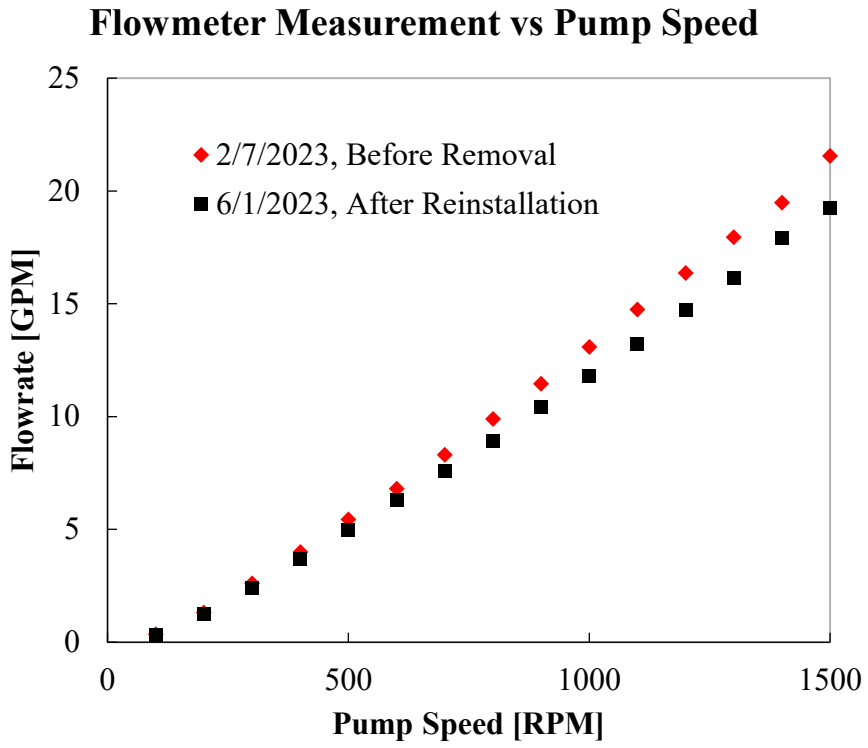

Figure 50: Measured sodium flowrate as a function of pump speed in the THETA primary system. As can be seen, there is a marked reduction in the measured flowrate, which is directly proportional to induced voltage in the electromagnetic flowmeter. Poor wetting, resulting in poor electrical conductivity on the inner pipe wall of the flowmeter, is suspected as a result of removing/replacing the test article.

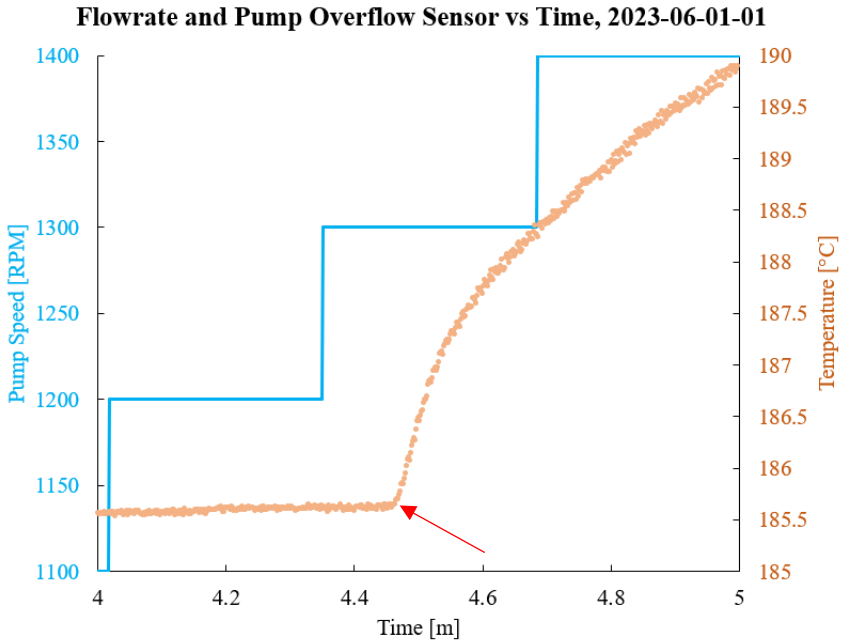

Figure 51: Pump speed and pump leakage thermocouple temperature (Figure 7) as a function of time. Pump maximum speed before leakage the same as before removal from system (Figure 14) suggesting the pump behavior/performance is similar. Red arrow shows where sodium touches the overflow thermocouple indicating a leak out of the top of the column pipe surrounding the pump shaft.

2.6.2. Stratification Testing

A testing campaign to characterize the improvement in thermal performance of the insulated core and IHX outlet was completed. This testing repeated stratification testing described in section 2.1.1. Plots showing hot and cold pool temperatures as a function of time for identical tests performed before and after the installation of the cold pool component insulation can be found in Figure 52. The thermal hydraulic parameters for these tests match Test #10 in Table 1. As can be seen in the right plot of Figure 52, when the core and IHX outlet insulators are backfilled with 4 PSIG argon, the sodium hot and cold pools possess significantly more stratified temperature fields. This is due principally to the reduced thermal conduction from the core to the cold pool. Additionally, in these tests the bottom IHX outlet window was opened, the insulated IHX outlet barrel reduces the amount of thermal conduction at the top of the IHX outlet. Thus, the relatively warm sodium in the IHX outlet is able to be injected into the bottom of the cold pool with less heat transfer, creating a more stratified cold pool.

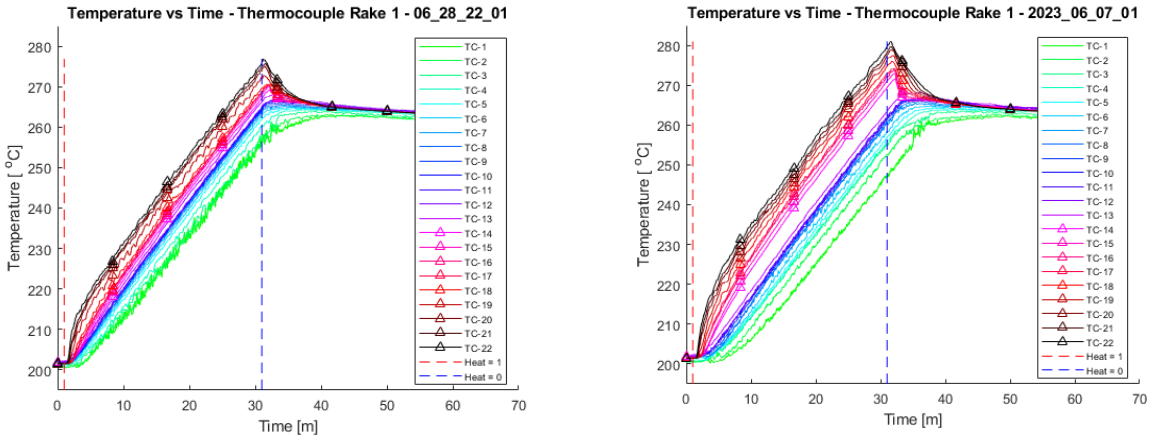

Figure 52: Temperature response during a thermal stratification transient test in THETA. The test on the left was performed before the addition of thermal insulation to the core and IHX outlet. The test on the right was performed with the core and IHX outlet insulation assemblies backfilled with 4 PSIG argon. Conditions for tests included as Test #10 in Table 1. Thermocouples are part of a single vertical multi-junction probe spanning the cold and hot pools. Thermocouples are numbered in sequential order starting with TC-1 at the bottom of the cold pool. TC-14-22 are in the hot pool and include a triangle marker on the plotted line for clarity. As can be seen a vertical red dotted line indicates the core electrical power being turned on and the blue dotted line indicates the core electrical power being turned off.

3. Secondary System Development

3.1. Intermediate Heat Exchanger

The sodium-to-sodium intermediate shell and tube heat exchanger (IHX) which transfers heat from the primary to the secondary system was fabricated, Figure 53. Instrumentation, including a 16-junction thermocouple probe and a capillary tube for an optical fiber temperature sensor, were both installed on the shell side of the IHX, Figure 54. The IHX was installed after inserting THETA with the insulated cold pool components (as opposed to installing the IHX onto THETA when it was removed) in order to facilitate testing of the upgraded primary system without the pressure drop from the tubes of the IHX. Therefore, a glovebag was used to facilitate insertion of the IHX into the primary system under an inert cover gas, Figure 55.

Figure 53: Photos at the IHX manufacturer before accepting the assembly. A helium leak check was performed under vacuum, as seen on left.

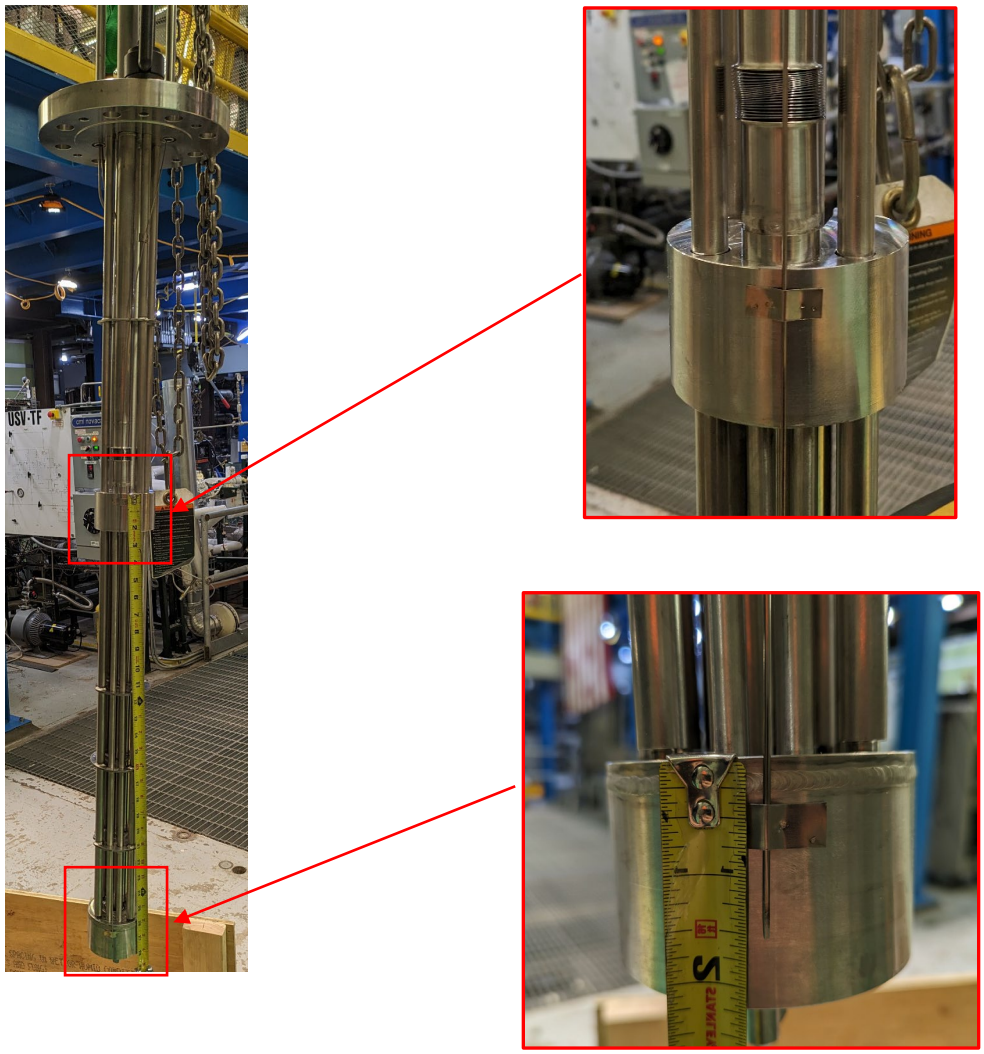

Figure 54: Photos showing the location of tack welds securing a 1/16” outer diameter 316SS capillary tube which will house a distributed optical fiber based temperature sensor.

Figure 55: Photos showing the installation of the IHX with the use of the overhead crane and a custom glovebag. On the left the glovebag is being cinched shut with a custom clamp as the glovebag is being inerted with argon. On the right the assembly is being inserted into THETA.

3.2. Secondary System Support Structure

The secondary system support structure was installed- consisting of a vertical 9.5' tall member that was bolted to the METL mezzanine structure and two horizontal members that were affixed to the building 308 high bay wall, Figure 56. After installing the structure and completing the installation of all of the secondary system components and piping it was discovered that the building 308 bridge crane, which is supported by the same I-beams that compose the structure of the high bay, imposed a significant amount of impulse force into the THETA secondary system support structure, through the support structure horizontal members. This created unacceptable force and oscillatory motion in the secondary system components. Thus, in order to isolate the support structure from the bridge crane, angled members were designed to replace the horizontal supports. The angled supports were fixed to the METL mezzanine which is bolted to grade, instead of the building, Figure 56. The THETA secondary support structure is now sufficiently isolated from the bridge crane motion. Additionally, all of the nondestructive testing of the secondary system was performed after the upgraded support structure was installed- no damage from the bridge crane oscillation was detected in the piping or components.

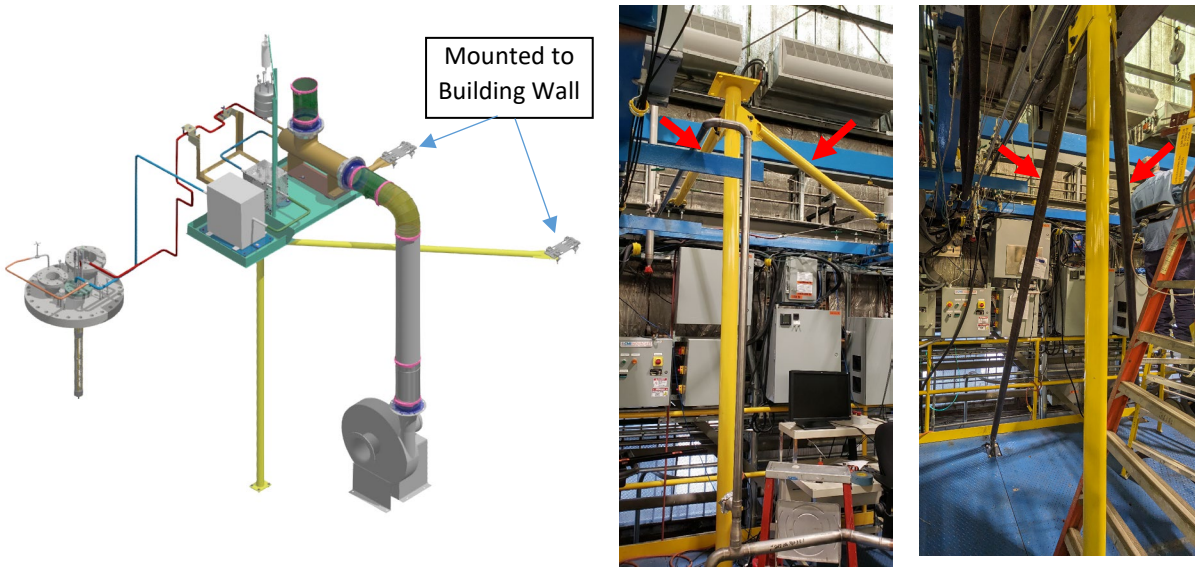

Figure 56: Installation of the THETA secondary support structure. Initially, the support structure was composed of horizontal members which bolted to a building 308 wall I-beam, as shown in left and middle pictures. These members were replaced with angled supports bolted to the METL mezzanine, which is isolated from the building, right picture.

3.3. Sodium-to-Air Heat Exchanger

Mineral insulated cable heaters were installed on the sodium-to-air heat exchanger (AHX), Figure 57, and the heat exchanger was insulated and installed on the secondary system support structure, Figure 58. Custom graphite sliding supports were installed on the feet of the AHX to reduce the sliding friction of the assembly, as required by ASME B31.3 analysis, Figure 57. The AHX blower and associated ductwork was also installed, Figure 59.

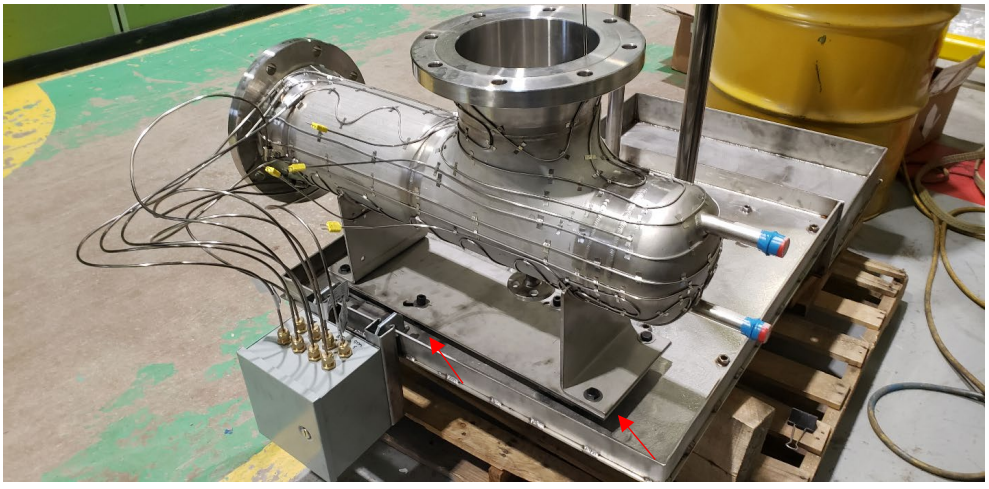

Figure 57: Sodium-to-air heat exchanger with mineral insulated trace heaters installed, before insulation. Graphite sliding pads were installed and are highlighted here with red arrows.

Figure 58: AHX installed on the secondary component support platform along with flowmeter and pump. The heat exchanger, flowmeter and pump were secured to the platform and hoisted as one unit to mount to the platform to the vertical support column. The components were then unbolted to allow for thermal expansion as required by ASME B31.3 piping analysis

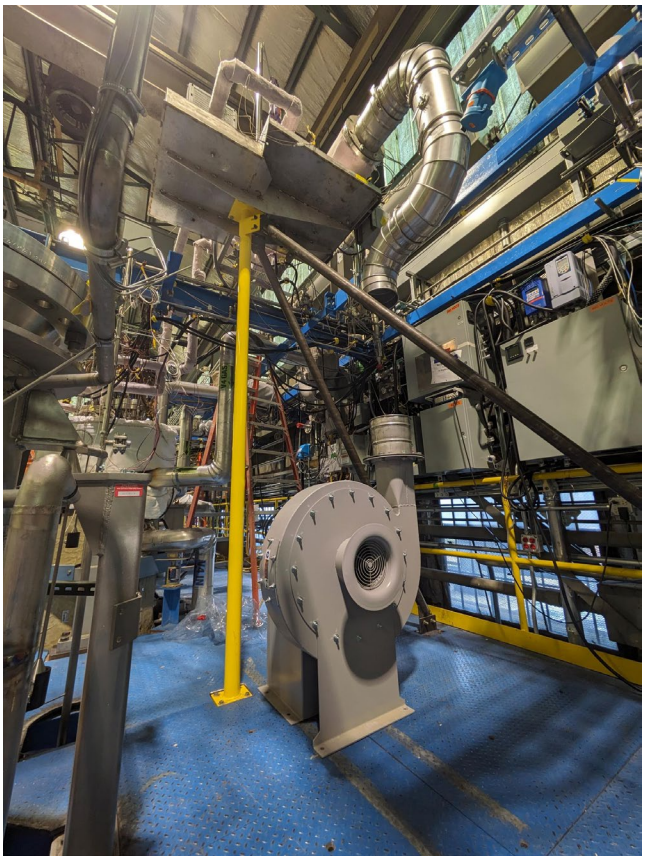

Figure 59: AHX blower installed on mezzanine. 9” stainless steel ducting being installed.

3.4. Electromagnetic Flowmeter and AC Conduction Pump

The secondary system electromagnetic flowmeter and AC conduction pump were installed on the support structure, Figure 58 and Figure 60. All of the AC conduction pump control and data acquisition systems were installed, Figure 61.

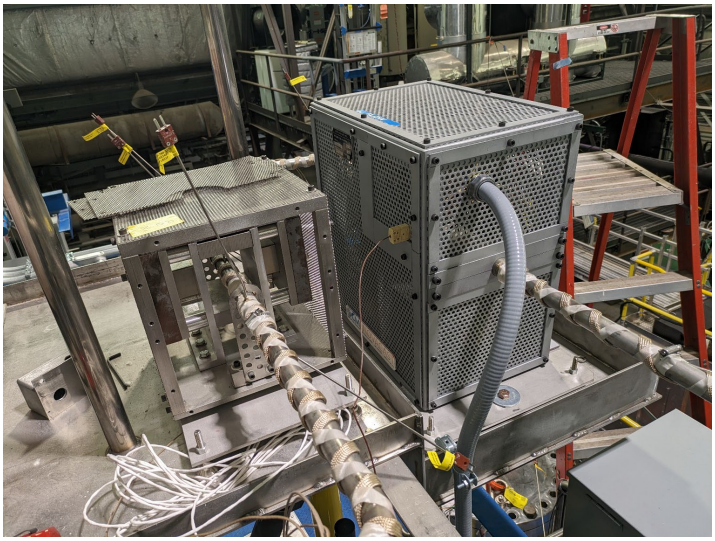

Figure 60: THETA ANL designed secondary permanent magnet based installed, left, in series with AC conduction pump, on right.

Figure 61: Three electrical cabinets installed for AC conduction pump.

3.5. Process Piping

The secondary system process piping was installed, consisting of ¾" and ½" SCH40 316/L dual certified and 316H stainless steel piping Figure 3. Nondestructive examination of all the welds was performed, Figure 62. A mass spectrometer leak detection was performed by pulling a vacuum of 14 millitorr on the piping and secondary components. No detectable leaks above 1<E-8 atm-cc/sec were measured with helium tracer gas. Dye penetrant examination was also performed on the welds by Argonne's Central Shop's quality assurance department. In addition, all piping welds were radiographed; some of the piping sections were able to be bench top welded which facilitated radiography to be performed offsite. However, in order to complete the piping assembly, there were 24 field welds that were required to be radiographed onsite. ANL engineers coordinated with an outside contractor to perform the weld radiography. The contractor performed the analysis on the radiograph films in addition to a qualified ANL senior welding engineer. Two of the field welds were determined to be unacceptable due to misalignment of the piping; these welds were replaced, and radiography performed again to ensure they passed.

Figure 62: Photos of the nondestructive examination being performed on the THETA secondary system including radiography (left and left center), dye penetrant testing (right center) and mass spec. leak detection (right).

Following the passing of all nondestructive examination, process heaters and associated control thermocouples were installed. The secondary system was split into 15 heating zones with two process control thermocouples located at strategic points along each zone to facilitate localized control of heat up, which is especially important when re-heating the system after draining and freezing as any trapped volumes of sodium, such as in the IHX which cannot be drained, must be heated from the "outside-in" to eliminate any chance of sodium thermal expansion related stress on the piping, Figure 63. The secondary system was then insulated using an initial 1" layer of alumina based Cerawool followed by two layers of ¼" thick Pyrogel XTE, Figure 64, Figure 65.

A secondary system heater control system was fabricated which uses Schneider Electric Mini-8 programmable logic controllers to control heat distribution in the 15 piping zones via solid state relays,

Figure 66. The Mini-8 is an industrial grade controller ideal for reliable heater control and is compatible with Modbus TCP/IP facilitating easy communication with the existing THETA Labview control software.

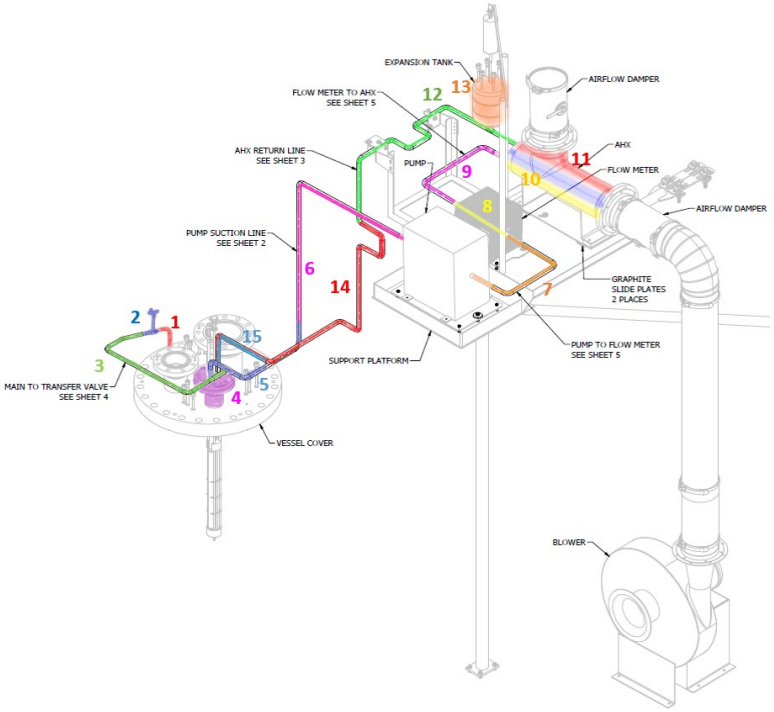

Figure 63: Secondary system heater zones 1-15

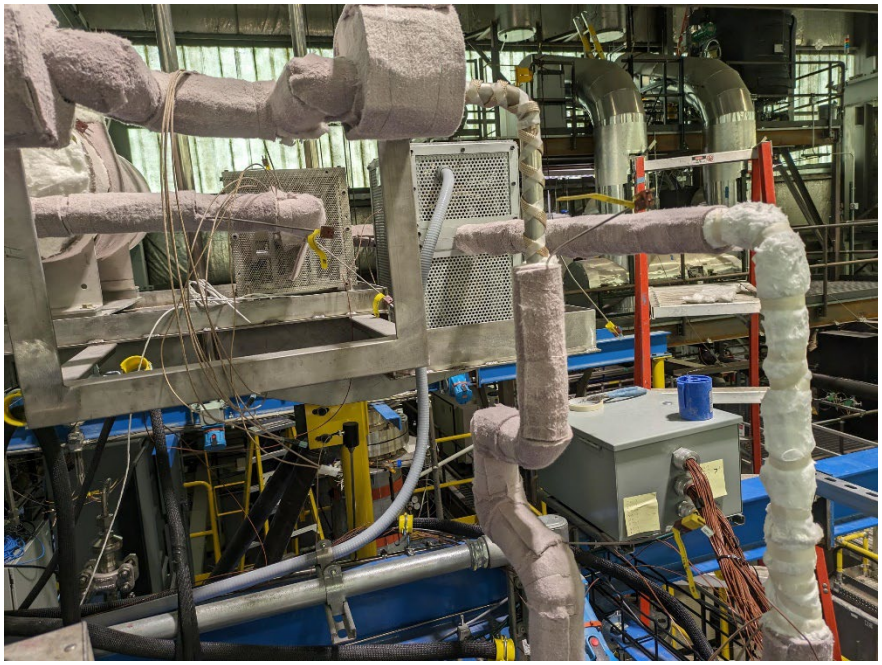

Figure 64: THETA secondary system process control heaters, white Cerawool insulation and purple Pyrogel XTE insulation being installed.

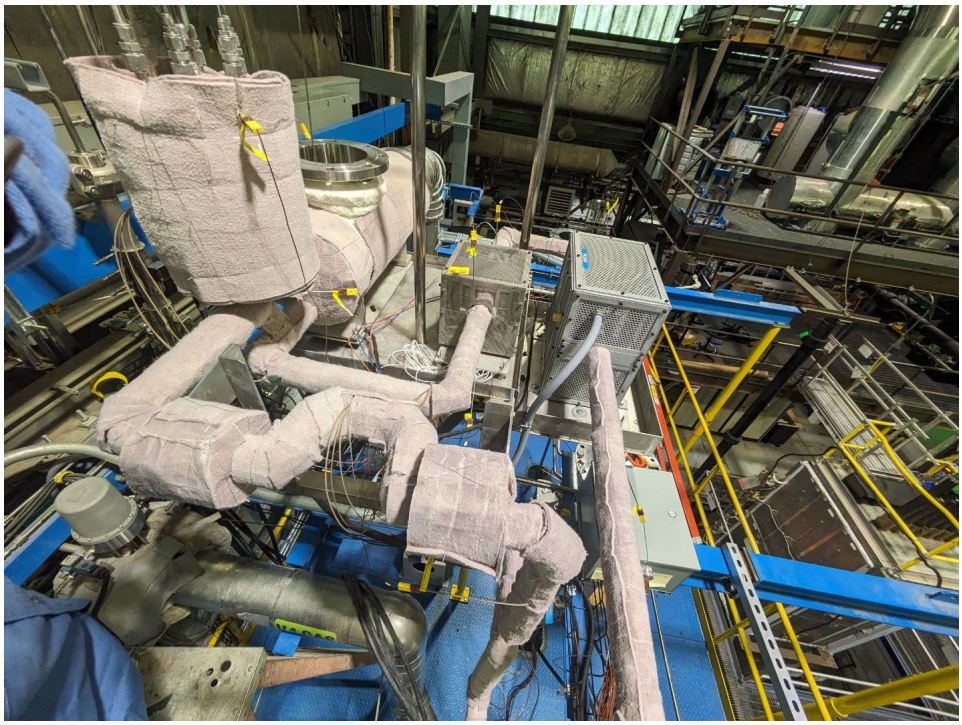

Figure 65: Photos of the THETA secondary system with insulation installed.

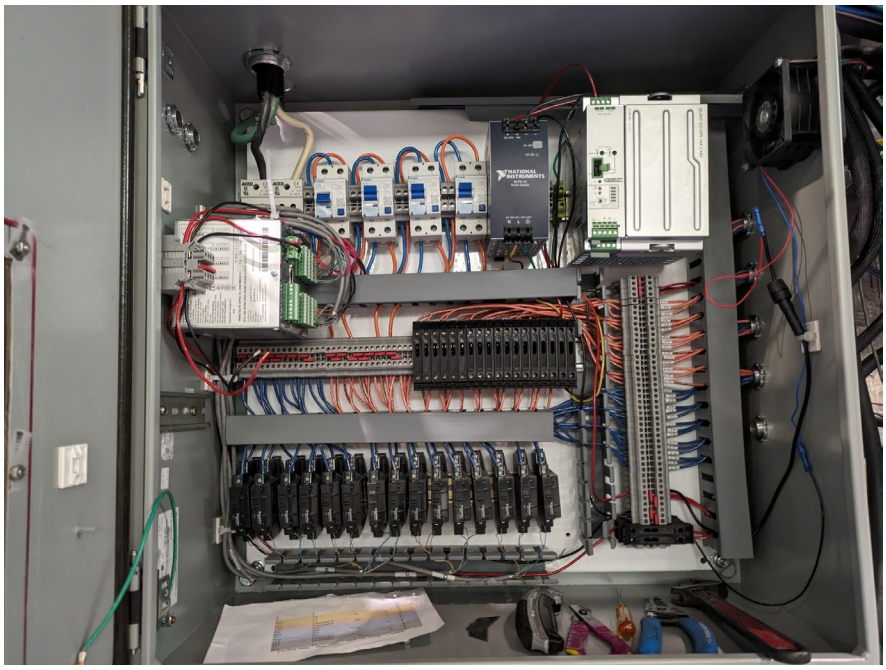

Figure 66: Photo of the THETA secondary system heater control system during fabrication

3.6. Expansion Tank

The expansion tank was welded into the piping assembly. A pipe hanger was selected using CAESAR-II pipe stress software that was used to support the expansion tank, and below piping, via a weld tab on the top of the expansion tank. The expansion tank possesses (6) ½" VCR ports that were each outfitted as follows:

1. Vacuum/gas line to control the vapor space of the expansion tank, leading to the expansion tank manifold, Figure 67.
2. Measurement thermocouple extending into the sodium space of the piping tee below the expansion tank to acquire a wetted sodium temperature of the hot sodium entering the AHX.
3. Measurement thermocouple to acquire sodium temperature in the expansion tank.
4. Measurement thermocouple to acquire vapor temperature in the expansion tank.
5. Conductivity level sensor to acquire a discrete level measurement at 3.8" above the bottom of the expansion tank, Figure 68, Figure 69.
6. Conductivity level sensor to acquire a discrete level measurement at 5.8" above the bottom of the expansion tank.

As can be seen in Figure 67, The expansion tank gas manifold allows the operator to tie the expansion tank gas space into the primary system gas space, set an independent gas space pressure, relieve pressure at a set point to facilitate system filling, pull vacuum on the system or vent the system. The line from the manifold to the expansion tank possesses an ASME pressure relief valve.

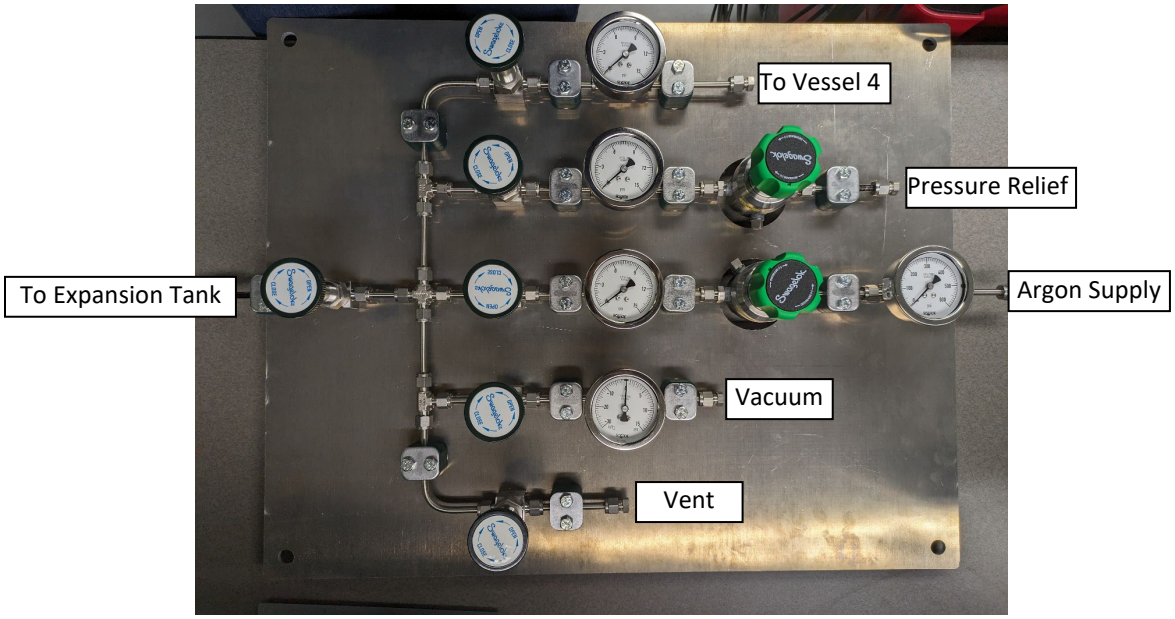

Figure 67: Expansion tank gas manifold

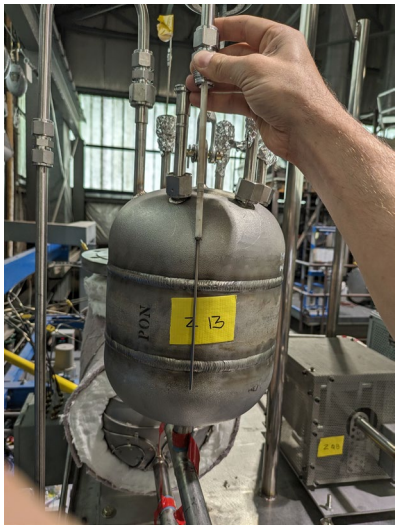

Figure 68: Expansion tank without trace heat or insulation showing the relative position of the lower conductivity probe level sensor.

Figure 69: Photo showing the two conductivity probe level sensors installed in THETA. These sensors were designed in-house and fabricated by an outside vendor.

4. Conclusions

Testing of the THETA primary system was completed this fiscal year. It was found that thermal conduction between the core and IHX outlet and the cold pool was too great to produce useful validation data for liquid metal cooled reactor systems code. Therefore, THETA was removed to facilitate the installation of thermal insulation on these components. Removing the test article necessitated the use of the 28” Flexicask, for the first time. The carbonation process was used to treat the residual frozen sodium on THETA. Solid sodium remained in the lower piping of THETA, resulting in damage to a flexible expansion pipe as a result of volumetric expansion during carbonation. THETA was disassembled as much as feasible to facilitate cleaning of the remaining solid sodium. THETA was then reassembled and the Flexicask was used to re-insert THETA. Testing was then performed with the upgraded insulation and the results suggest the improvements were effective. The THETA secondary system was then installed which involved the installation of a secondary support structure. Next fiscal year, the secondary system will be filled with sodium and a testing campaign will be completed which includes the balance of plant.

Acknowledgements

The authors would like to acknowledge Daniel Andujar of the METL team for all his hard work and dedication to supporting the THETA test article. In addition, the authors would like to thank Argonne Central Shops employees for their quality craftsmanship and support, including Bill Toter, Mark Rooney, Dan Berkland, Tyler Anderson, Kristi Wood and Jonathan Torres.

This work is funded by the U.S. Department of Energy Office of Nuclear Energy's Advanced Reactor Technologies (ART) program. A special acknowledgement of thanks goes to Ms. Kaatrin Abbott, Fast Reactor Program Manager for the DOE-NE ART program, Dr. Bo Feng, the National Technical Director for Fast Reactors for the DOE-NE ART program, and to Mr. Bradley Tomer, Acting National Technical Director for the National Reactor Innovation Center for their consistent support of the Mechanisms Engineering Test Loop and its associated experiments, including THETA.

References

[1] M. Weathered, et al, "Thermal Hydraulic Experimental Test Article – Status Report for FY2019 Rev. 1," 2019 doi: 10.2172/1570468

[2] M. Weathered, et al, "Thermal Hydraulic Experimental Test Article (FY21 Final Report)," 2021, doi:10.2172/1825485

[3] M. Weathered, D. Kultgen, E. Kent, J. Rein, and C. Grandy, "Thermal Hydraulic Experimental Test Article – Fiscal Year 2022 Final Report," Lemont, 2022.

[4] J. McCay, et al, "Comparison of Sodium Stratification in CFD to Experimental Data from the Thermal Hydraulic Experimental Test Article," NURETH-20 Conference, August 2023, Washington, D.C.

[5] D. Kultgen, C. Grandy, E. Kent, and M. Weathered, "Mechanisms Engineering Test Loop – Phase I Status Report – FY2018," 2018.

[6] M. Weathered, C. Grandy, M. Anderson and D. Lisowski, "High Temperature Sodium Submersible Flowmeter Design and Analysis," in IEEE Sensors Journal, vol. 21, no. 15, pp. 16529-16537, 1 Aug.1, 2021, doi: 10.1109/JSEN.2021.3079713.

[7] G. Turner, "Liquid Metal Flow Measurement (Sodium) State-of-the-Art Study," LMEC-Memo-68-9, June 1968

Nuclear Science & Engineering
Argonne National Laboratory
9700 South Cass Avenue, Bldg. 206
Argonne, IL 60439

www.anl.gov